

# Helicopter Triggered Lightning in Norway

Utilizing model and observational data to investigate cases of reported lightning to aircraft in Norway

Johannes Tobiassen Langvatn



Thesis submitted for the degree of  
Master of science in Meteorology  
60 Credits

Department of Geosciences  
Faculty of Mathematics and Natural Sciences

UNIVERSITY OF OSLO

July 31, 2020

© 2020 Johannes Tobiassen Langvatn

Helicopter Triggered Lightning in Norway: Utilizing model and observational data to investigate cases of reported lightning to aircraft in Norway

This work is published digitally through DUO – Digitale Utgivelser ved UiO

<http://www.duo.uio.no/Printed>: Representralen, University of Oslo

All rights reserved. No part of this publication may be reproduced or transmitted, in any form or by any means, without permission.

# Abstract

Helicopters are sometimes hit by lightning when flying offshore along the coast of Norway. Often, the helicopter's presence is what triggers the lightning strike, and this phenomenon is called Helicopter Triggered Lightning (HTL). These lightning strikes present both an economic and a safety risk to offshore operators. The current forecast for HTL in Norway was introduced in 2016, and named Helicopter Trigger Index. Since then, cases of HTL have been reported, which implies that the introduction of the forecast did not provide a robust enough forecast to prevent all HTL events.

This thesis provides a thorough investigation into reported incidents of triggered lightning in Norway. In addition, the available theoretical models used as a basis for the HTL forecast are assessed. The thesis reaffirms the importance of the  $0^{\circ}\text{C}$  isotherm in forecasting HTL. It is found that the Helicopter Trigger Index might be improved upon by increasing the weighting of current precipitation and temperature parameters when computing the index. It is also concluded that a possible predictor of HTL is wind directed on-shore, which is a parameter not included in the index today.

The study found also an error in the forecasting algorithm, leading to an overestimation of risk related to offshore flying. It was found that the correction of the algorithm error would increase the forecast skill, especially on the northern facing coast of Norway.

# Acknowledgements

It is with great honor I now present the product of two amazing years as a Master student. This thesis could not have been completed without considerable help from various people around me. Special thanks goes to my supervisors Trude Storelvmo and Morten Kølitzow. For their supervision and helpful guidance, and not least their constructive criticism of my writing style. I would be remiss not to thank Johanne Mehren for tipping me off to the opportunity of this project, and of course for her friendship and jokes (Even or maybe especially those on my behalf).

I am of course indebted to Martin Boie Christiansen and Glenn Christiansen for their help and interest in this project. Their insights into the world of helicopters have been essential. I still am awaiting their offer to let me fly in one of their helicopters.

The thesis was also written in a time of great global turmoil, as the world was hit by the COVID-19 pandemic. This in turn leads me to thank the Rian Julsrud family for their hospitality in letting me isolate from the rest of the world in their cellar. It is not an understatement that I have learned and continue to learn immensely by our talks at the coffee- and dinner tables.

The list of people who I owe thanks to contains a myriad of names. I would love to list them all but, the paper usage would not be defensible. Instead I would thank a special few who is not aforementioned: My mother and father, my American proofreader and friend Jonah, my brothers Tobias and Alphonse, and the Ingeborg(s)

**Johannes Tobiassen Langvatn**

**July 2020**

# Contents

<b>Abstract</b>	<b>i</b>
<b>Acknowledgement</b>	<b>ii</b>
<b>List of Figures</b>	<b>viii</b>
<b>List of Tables</b>	<b>ix</b>
<b>Acronyms</b>	<b>xi</b>
<b>1 Introduction and Motivation</b>	<b>1</b>
<b>2 Theory and Background</b>	<b>5</b>
2.1 Convection and cloud creation . . . . .	5
2.2 Cloud electrification . . . . .	6
2.3 Natural lightning . . . . .	7
2.3.1 Winter lightning . . . . .	8
2.4 Helicopter Triggered Lightning . . . . .	9
2.5 Fixed wing Triggered Lightning . . . . .	11
2.6 Helicopter Trigger Index . . . . .	12
2.6.1 Precipitation error in HTI . . . . .	14
<b>3 Methods</b>	<b>17</b>
3.1 Models . . . . .	17
3.1.1 Numerical Weather Prediction - model . . . . .	17
3.1.2 Reanalysis - model . . . . .	18
3.2 Data . . . . .	18
3.2.1 Incidents from Avinor . . . . .	18
3.2.2 Meteorological aerodrome report . . . . .	19
3.3 Composite plots . . . . .	20
3.4 Decomposition of HTI . . . . .	20

3.5	Interpolation . . . . .	20
3.6	Model limitations . . . . .	21
3.6.1	Temporal uncertainty . . . . .	21
3.6.2	Pressure level vs Model level interpolation . . . . .	21
3.6.3	Loss in data due to archiving . . . . .	23
<b>4</b>	<b>Results and discussion</b>	<b>25</b>
4.1	Analysis of Avinor triggered lightning data set . . . . .	25
4.2	Meteorological phenomena related to triggered lightning . . . . .	28
4.2.1	METAR observations . . . . .	28
4.2.2	Temperature during triggered lightning events . . . . .	32
4.2.3	Typical pressure pattern during triggered lightning events . . . . .	32
4.2.4	Vertical velocity during triggered lightning events . . . . .	35
4.2.5	Different types of precipitation for triggered lightning events . . . . .	37
4.2.6	Why are there more HTL near Flesland than near Sola? . . . . .	41
4.3	Implications of precipitation error in HTI . . . . .	42
4.4	Decompositional analysis of triggered lightning incidents . . . . .	45
<b>5</b>	<b>Conclusions</b>	<b>51</b>
5.1	Are there still cases of Helicopter Triggered Lightning in Norway? . . . . .	51
5.2	What meteorological phenomena are present during triggered lightning incidents? . . . . .	51
5.3	In what ways can the HTL forecast be improved? . . . . .	52
	<b>Bibliography</b>	<b>53</b>
<b>A</b>	<b>Additional figures</b>	<b>53</b>
A.1	HTI before and after fix of erroneous forecast . . . . .	53
<b>B</b>	<b>Airport names and geographical zones</b>	<b>63</b>
B.1	ICAO-codes . . . . .	63

# List of Figures

1.1	Seasonal variation of helicopter cases, showing no cases in May to September. Data is produced from Lande, 1999 and Wilkinson et al., 2013. Legend notes time-periods and amount of cases in each study. . . . .	2
2.1	Simple diagram illustrating the two main categories of lightning. A shows an Intracloud discharge (IC), this could be between different storm cells or between different charge areas of the same storm cell. B shows a Cloud-to-ground discharge (CG), the polarity is defined by the charge change of earth. Negative cloud-to-ground (-CG) is defined by increase of negative charge at ground, and so positive cloud-to-ground (+CG) is defined by decrease of negative charge (increase in positive) at ground . . . . .	9
2.2	Outside air temperature (OAT) adapted from earlier HTL-studies, showing the 0 and -2 degree temperatures to be most represented in HTL-cases . . .	10
2.3	Illustration of different models for aircraft triggering. A shows the normal trigger situation, where the electrical discharge is grounded into the oppositely charged aircraft. B shows the situation where the aircraft is only acting as a pathway to the ground (Here ocean or land) . . . . .	11
2.4	Sub-index value for different input for the four parameters used in the calculation of HTI . . . . .	13
2.5	Screenshot from <a href="https://www.ippc.no">https://www.ippc.no</a> for 21. of January 2020, showing the HTI-forecast with 8 hour lead-time after midnight. The blue thunder-cells show another forecast-product from MET, forecasting risk for natural lightning. A plane was hit by lightning, and was therefore diverted from flying into Bodø during this forecasts valid time. . . . .	15
3.1	Difference between model level and pressure level interpolations for a) Temperature and b) geopotential height. The temperature is found by geopotential height as discussed in Section 3.5, such that these variables are not independent. . . . .	22

3.2	Difference of ERA5 and MEPS temperatures using pressure level interpolation to case height. . . . .	22
4.1	Seasonal variation of helicopter cases, showing no cases in June to September. Same as Figure 1.1, with cases looked at in this study added to it. Older data is produced from Lande, 1999 and Wilkinson et al., 2013. Legend notes time-periods and amount of cases in each study. . . . .	25
4.2	Temperature in fixed-wing and helicopter cases (interpolated from ERA5 pressure levels) . . . . .	26
4.3	Cases per year from the Avinor data set, delineated between cases before operational forecast was in place in the left figure, and after operational forecast was used in the right figure. . . . .	27
4.4	Zonal division of helicopter cases . . . . .	27
4.6	Frequency of different categories of METAR-phenomenon for Helicopter and Fixed wing cases, included are only cases where airport had a METAR-report that was taken by a non-automatic system. Note that SH also include VCSH . . . . .	30
4.7	Percentage of METAR-reports involving at least one of the meteorological phenomena at Hammerfest, Ørlandet, Flesland, Sola, and Gardermoen airports. Selection is based on geographical variation and representation. . . .	31
4.8	Temperature composites for both HTL and FwTL cases in different geographical zones. Included are only cases for which height information was provided in the Avinor data set. The temperature was found by interpolating to the correct height as described in Section 3.5 . . . . .	34
4.9	Same as Figure 4.8, but for only the biggest airports. . . . .	35
4.10	Vertical velocity composites for both HTL and FwTL cases in different geographical zones. Included are only cases for which height information was provided in the Avinor data set. The velocity was found by interpolating to the correct height as described in Section 3.5 . . . . .	36
4.11	Same as Figure 4.10, but for only the biggest airports. . . . .	37
4.12	Large scale precipitation composites for both HTL and FwTL cases in different geographical zones. Included are cases where height information was <i>not</i> provided in the Avinor data set. . . . .	38



4.13	Same as for Figure 4.12, but for only the biggest airports . . . . .	39
4.14	Convective precipitation composites for the different zones . . . . .	40
4.15	Convective precipitation composites for the biggest airports. . . . .	41
4.16	Frequency of HTI-risk levels during HTL-season (October-April), before and after fixing the erroneous forecast, for selected airports. . . . .	43
4.17	Frequency of HTI-risk given observed meteorological-phenomenon during HTL-season (October-April), for the three northernmost coastal airports: Hammerfest (ENHF), Bodø (ENBO), and Brønnøysund (ENBN) . . . . .	44
4.18	Frequency of HTI-risk given observed meteorological-phenomenon during HTL-season (October-April), for the three northwestern coastal airports: Ør- landet (ENOL), Kristiansund (ENKB), and Florø (ENFL) . . . . .	45
4.19	Contributions from the different sub-indices, for Helicopter cases during the operational forecast. X-axis is height of incident in feet. Black on yellow is correction made by using the hourly precipitation instead of accumulated precipitation. Included are only cases from Avinor data set where position and height was available, for cases after November 2016. . . . .	47
4.20	Same as 4.19, but clearly delineated between the sub-indices . . . . .	48
4.21	Contributions from the different sub-indices, for Fixed wing cases during the operational forecast. X-axis is height of incident in feet. Black on yellow is correction made by using the hourly precipitation instead of accumulated precipitation. Included are only cases from Avinor data set where position and height was available, for cases after November 2016. . . . .	49
4.22	Same as 4.21, but clearly delineated between the sub-indices . . . . .	50
A.1	North zone, cases with HTI-value before and after precipitation change . .	53
A.2	North West zone, cases with HTI-value before and after precipitation change	54
A.3	West zone (First part), cases with HTI-value before and after precipitation change . . . . .	55
A.4	West zone (Second part), cases with HTI-value before and after precipitation change . . . . .	56
A.5	South zone, cases with HTI-value before and after precipitation change . .	57
A.6	Cases where exact position is not-known, with HTI-value before and after precipitation change . . . . .	58

A.7	Cloud cover composites for both HTL and FwTL cases in different geographical zones. Included are cases where height information was <i>not</i> provided in the Avinor data set. . . . .	59
A.8	Cloud cover composites for both HTL and FwTL cases for only the biggest airports. Included are cases where height information was <i>not</i> provided in the Avinor data set. . . . .	60
A.9	Frequency of the different risk levels of HTI during HTL-season (October-April), before and after correction of erroneous use of accumulated precipitation. Also shown is the absolute difference between the original and fixed frequencies. . . . .	61
A.10	Operational risk levels and description of procedures during reported risk for HTI. As reported to the helicopter operators. Note: Brown risk level has been consequently called Orange through the whole thesis. . . . .	62
B.1	Zones used in this thesis, with used METAR-stations in white, and airports with at least one incident in red. . . . .	64

# List of Tables

3.1	Data available for each case in the Avinor-dataset. Note that there is one helicopter case where height is not known, but position is. . . . .	19
3.2	METAR-codes for reporting weather phenomena. The last four categories includes a numerical value for how much of the cloud is covered by clouds, OVC refers to total cloud cover, FEW refers to one to two eights of sky is cloud . . . . .	19
4.1	Average traffic, accumulated lightning activity, and cases within $0.5^\circ (\approx 50km)$ radius of the three biggest Norwegian airports. . . . .	42
4.2	Amount of cases forecast in each risk category based on the 11 Helicopter cases in Figure 4.19. A Red risk is counted in Orange, and Yellow. . . . .	47
4.3	Amount of cases forecast in each risk category based on the 34 Fixed wing cases in Figure 4.21. A Red risk is counted in Orange, and Yellow. . . . .	49
B.1	ICAO-code for the airports and helipads used in this thesis. . . . .	63



# Acronyms

**CG** Cloud-to-ground discharge. v, 8–10

**ECMWF** European Centre for Medium-Range Weather Forecasts. 18

**ERA5** ECMWF atmospheric reanalysis. 3, 18, 19, 21, 52

**FwTL** Fixed wing Triggered Lightning. vi, viii, 2, 3, 5, 11, 20, 26, 28, 34, 36, 38, 42, 46, 59, 60

**HTI** Helicopter Trigger Index. v, vii, viii, 2, 5, 12–14, 20, 23, 25, 32, 42–46, 51, 52, 61, 62

**HTL** Helicopter Triggered Lightning. v–viii, 1–3, 5, 7–12, 14, 17, 20, 21, 25, 26, 28, 32, 34, 36, 38, 42–45, 51, 52, 59–61

**IC** Intracloud discharge. v, 8, 9

**MAD** mean absolute difference. 21

**MEPS** MetCoOp ensemble prediction system. 3, 17–19, 21, 52

**METAR** Meteorological aerodrome report. vi, ix, 19, 28, 30, 31, 42, 51

**MetCoOp** Meteorological Cooperation on Operational Numeric Weather Prediction. 3

**NWP** Numerical weather prediction. 2, 17, 18

**OAT** Outside air temperature. v, 9, 10, 19



# 1 Introduction and Motivation

Helicopters are a vital part of the transport of personnel to offshore installations along the Norwegian coast. Offshore personnel report fear of being involved in helicopter incidents. They also experience unease from flying in turbulent and bad weather (Wasilewska, 2019). These weather types may be causal to lightning incidents, as suggested in earlier work (e.g. Lande, 1999; Wilkinson et al., 2013; Smart, 1997). It has been estimated that the repair cost due to a lightning strike to a helicopter was on the order of 100,000 U.S. Dollars (Lande, 1999). The incident rate can be estimated from earlier data sets to about 2.05 per year for Norwegian operators in the period 1979-1999. This would then result in the accumulated economic loss of about 4 300 000 U.S. Dollars for the Norwegian operators. This potential in economic loss is severe in itself, but added onto this is also the danger helicopter pilots and passengers are put in, when the aircraft is hit by lightning. There are two major helicopter crashes related to lightning in the last 30 years (1995 and 2001) as discussed later in this section. By comparison, in the same period there has been only one airplane crash among the Norwegian operators (transport, 2007), even though airplanes are flying much more frequently in Norway. It is therefore imperative to exhaust the investigation into the causes of and possible ways to prevent helicopter related incidents.

Lightning strikes can in various ways be the cause of helicopter incidents. These incidents include events when rotors have been destroyed, as in the case of Flight 56 in 1995 (Smart, 1997). Sometimes a breakdown of the structural integrity of a rotor by lightning is not discovered right away, but can still be serious. For example, a lightning strike in 1999 is believed to have caused a fatal crash in 2002 (Smart, 2005). Incidents of less fatal variety include disruption to electrical equipment (Table 2. in M. Uman and V. Rakov, 2003).

Helicopters flying offshore are in practice only hit by lightning in wintertime (See Figure 1.1). These incidents usually happen even though there is no lightning activity in the area beforehand. (Helicopter pilots naturally avoid regions with lightning activity.) When the helicopter is hit by lightning in an area without lightning activity it is referred to as Helicopter Triggered Lightning (HTL) (e.g. Lande, 1999; Wilkinson et al., 2013). The triggering refers to the helicopter initiating the lightning strike by its presence, meaning that without the

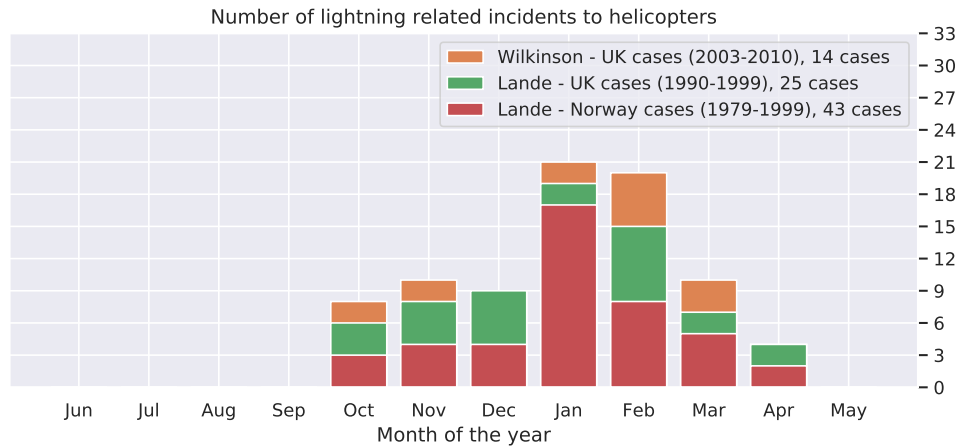


*Figure 1.1: Seasonal variation of helicopter cases, showing no cases in May to September. Data is produced from Lande, 1999 and Wilkinson et al., 2013. Legend notes time-periods and amount of cases in each study.*

helicopter there would be no lightning strike.

The study of HTL had its peak around the turn of the century, due to two helicopter incidents related to lightning (1995 and 2002). The 1995 incident was a non-fatal incident. A lightning strike destroyed the main rotor of the helicopter, forcing the pilot to perform a landing in the ocean (Smart, 1997). The 2002 incident resulted in eleven fatalities and is believed to have been caused by internal damage to the helicopter’s main rotor back in 1997. The initial inspection of the rotor did not uncover any damage, causing the helicopter to be cleared for flight. This initial structural damage later resulted in failure of the main rotor, leading to the crash in 2002 (Smart, 2005). These events resulted in practical guidelines to helicopter pilots based on data from earlier incidents (Lande, 1999, Hardwick, 1999). Furthermore, the UK Met Office added numerical simulation and forecasting to these guidelines, with the introduction of Helicopter Trigger Index (HTI). This provided a more robust warning for helicopter pilots (Wilkinson et al., 2013). Since then, general Numerical weather prediction (NWP) forecasts have improved and continue to improve due to better physical understanding, more and higher quality observations, and increase in available computational power. This thesis aims to improve upon the understanding of the HTL phenomenon by using state-of-the-art model products as described in Section 3.1.

The author makes use of a novel dataset from Avinor containing reported incidents of both HTL and a similar phenomenon: Fixed wing Triggered Lightning (FwTL). FwTL is triggered



lightning involving planes and rockets, where the wings are fixed. FwTL, unlike HTL, is of less danger to both personnel and materials. Fixed wing aircraft are generally hit in the main body. Fuel and vital electronics are also better protected in fixed wing aircraft (Petrov et al., 2012). Helicopters are mainly hit through the rotor into the main body (Lande, 1999). Despite this difference in actual risk, both incidents are associated with non-negligible risk, and require thorough inspection of the aircraft after the fact.

To investigate atmospheric conditions during HTL and FwTL incidents, the ECMWF atmospheric reanalysis (ERA5) data set is utilized. Also used for this purpose is the operational MetCoOp ensemble prediction system (MEPS)<sup>1</sup>.

These are the research questions this thesis attempts to answer:

- Are there still cases of Helicopter Triggered Lightning in Norway?
- What meteorological phenomena are present during triggered lightning incidents?
- In what ways can the HTL forecast be improved?

The goal is to improve and strengthen the confidence in the current operational HTL forecast. Also under investigation is an error found in the algorithm used to produce the operational forecast where the accumulated precipitation, and not the intended hourly precipitation, was used in the operational forecast. This lead to a potential over-estimation of risk related to offshore flights.

---

<sup>1</sup>Meteorological Cooperation on Operational Numeric Weather Prediction (MetCoOp)



## 2 Theory and Background

Observation of lightning is a natural part of human history, from early man believing it to be caused by the wrath of deities, to the modern storm chaser utilizing radar observations of precipitation to get the best view of a storm. The scientific study of lightning, on the other hand, is relatively new. The first steps towards systematic study were the experiments performed by Benjamin Franklin, along with the development of the theory of electromagnetism. Only in the last century have we acquired the means to thoroughly investigate the electrical and meteorological mechanisms resulting in a thunderstorm. This is due to both more available measurements and better physical understanding. The measurements are made possible by aircraft being able to fly through storm clouds providing in-situ observations, and satellite imagery providing a view into the vertical composition and structure of clouds.

This chapter briefly explains cloud creation, cloud electrification and lightning, using this to describe what is known about what separates Helicopter Triggered Lightning and Fixed wing Triggered Lightning from natural lightning. Finally the Helicopter Trigger Index (HTI) is introduced and described.

### 2.1 Convection and cloud creation

Lightning occurs in storm clouds, and therefore an explanation of cloud creation mechanisms is necessary to understand why lightning occurs. One of the key components to cloud creation is an unstable atmosphere: an atmosphere where temperature decreases with height. Instability can be understood by recognizing that warm air is less dense than cold air, and thus buoyant in the colder surrounding air. When air rises, less pressure is exerted on it, since the atmosphere is densest at the surface. This lower pressure causes work to be done by the rising air, to expand to a new equilibrium. If the air rises fast enough for the expansion to be adiabatic, this work leads to a cooling of the air mass. This cooling slows the vertical movement due to less buoyancy.

However, if moisture is present at the surface, water vapor will be displaced upwards by this vertical movement. When the air mass is cooled by the expansion, the saturation vapor pressure decreases. Lower saturation vapor pressure favours more water in the condensed

phase, either as ice or water particles. Condensation of water vapor heats the ascending air, which causes more vertical movement. Thus, a dry atmosphere is inherently more stable than a humid atmosphere, as the lack of condensation would lead to equilibrium due to adiabatic cooling alone.

If temperatures are sufficiently low ( $\leq 0^{\circ}\text{C}$ ), the liquid water may freeze to ice crystals. The uncertainty here is due to the heat released when a crystalline surface is created: A typically sized liquid droplet requires a temperature of around  $-38^{\circ}\text{C}$  or lower to initiate homogeneous freezing (Lamb and Verlinde, 2011). This leads to relatively clean air containing super-cooled liquid droplets below bulk freezing temperature of  $0^{\circ}\text{C}$ . Alternatively, by introducing a surface which the structure can grow on (an ice nucleation particle), this reduces the energy released, thus raising the temperature requirement for freezing initiation up towards the melting temperature (Jeffery and Austin, 1997).

Convection is, by its very nature, a chaotic and stochastic process. Convection is the result of turbulent effects, and therefore it is hard to model and forecast. This is abated by use of ensemble prediction systems and fine scale convection-permitting models.

## 2.2 Cloud electrification

There are different theories in the still-open field of thunderstorms, pertaining to both the electrification mechanisms and the general electrical structure of thunderstorms. This is further complicated by the fact that there seem to be different mechanisms at work for different scales of storms.

There are two main mechanisms of electrification believed to be dominant (e.g. C. Saunders, 2008; Soula, 2012): inductive effects from hydrometeors falling and colliding in the fair-weather electric field present in the atmosphere (Harrison, 2012) and the electrochemical effects in water colliding with other water particles of different size and phase (e.g. Williams, 1991; Kallay, Drzymala, and Cop, 2015)

### **Inductive electrification**

There is a fair weather electrical field present in the atmosphere on the order of  $100\frac{\text{V}}{\text{m}}$  (e.g. Harrison, 2012). Any polarizable particle moving through this field will be polarized such that the negative charge is on the top and the positive charge is on the bottom. Thus, a water droplet or ice crystal falling as precipitation may selectively capture negative ions as they are attracted to the positive pole on the bottom of the particle. The positive ions will be repelled

by the same charge. This will then remove only one type of charge from the atmospheric layer and lead to a charge buildup. It can then be understood that if there are concurrent streams, one of precipitation falling faster than the updraft, and one of hydrometeors being carried aloft in the updraft, they would remove ions of opposite polarity at different heights such that you get a dipole or a more complex tripole structure (Stolzenburg, Rust, and Marshall, 1998). Thus, the inductive electrification mechanism requires a substantial number of hydrometeors to create enough charge for lightning to be produced. This is observed in thunderstorms with high amounts of precipitation and can happen in pure liquid clouds.

### **Non-inductive electrification**

Outside of a strong electrical field, one can still measure electrification from particle collisions between ice and water or over a freezing/melting ice surface. This effect, dubbed the Costa-Ribeiro effect in e.g. (Pinatti and Mascarenhas, 1967), is due to an electrical double layer at the ice-liquid interface (Kallay, Drzymala, and Cop, 2015). This causes a potential across the interface and the equalization of this potential leads to a charge reorganizing in the colliding particles. The resulting charge build-up is found to be heavily reliant on ambient temperature and cloud liquid water content (C. P. R. Saunders et al., 2006; Takahashi, Tajiri, and Sono, 1999).

When the electrification has happened, areas of dominant charges are created. To equalize the charge distribution, charge is transferred between these areas of different polarity. These discharges are what is observed as lightning.

## **2.3 Natural lightning**

To explain what separates Helicopter Triggered Lightning from other lightning, an explanation of natural lightning is appropriate. The *typical* lightning storm is created in summertime. It can generally be caused by solar radiation heating up the ground, creating an unstable atmosphere (V. A. Rakov and M. A. Uman, 2003). Alternatively, or in combination with this, an instability may be caused by colder air moving over less cold (warmer) areas. The "natural" lightning then refers to an instability and electrification process strong enough to create a lightning discharge from the clouds to the ground. This is on the order of  $10^6 \frac{V}{m}$  for dry air at surface pressure (V. A. Rakov and M. A. Uman, 2003), which is approximately  $100mC$  situated in a point charge  $1km$  away from the point of measurement. Typical values for charge density in thunderclouds are on the order of  $1 - 100 \frac{nC}{m^3}$ , though the total elec-

trical field is on the order of  $10^5 \frac{V}{m}$  (V. A. Rakov and M. A. Uman, 2003). The difference between the required electric field and measured electric fields requires a triggering event to initiate a lightning strike. In natural lightning, the triggering event is believed to be random plasma channels or leaders emitted from the strong electric field, explained thoroughly in V. A. Rakov and M. A. Uman, 2003. Lower air pressure and more available humidity (or other polarizable particles) increase the conductivity of the air and thus reduce the required electrical field for a lightning strike.

Lightning discharges in a thunderstorm can generally be divided into two categories (e.g. Lynn et al., 2011): Intracloud discharge (IC) and Cloud-to-ground discharge (CG), see Figure 2.1 for description and comparison. A CG is seen developing downwards before making contact with the ground. The stream of electrons developing downwards (Visible as a tree of characteristic jagged "lightning" shape) is what is referred to as a leader (V. A. Rakov and M. A. Uman, 2003). On the other hand, IC often does not have an observable leader, since the distance between charged parts of the cloud are closer to each other than to earth, and thus does not require a leader to trigger the strike.

### 2.3.1 Winter lightning

Winter lightning is a type of natural lightning specifically relevant to HTL in Norway, as discussed in the next section. It is a relatively well-studied phenomenon in Japan. Cold air from Siberia moves over the warm Tsushima current off the west coast of Japan, causing convection due to a strong temperature gradient between the cold air and the warm ocean. The supply of humidity from the seawater leads to formation of hydrometeors. The resulting convection has been shown to produce lightning strikes and thunderstorms during winter (Michimoto, 2007).

Winter lightning is also observed off the west coast of Norway (e.g March et al., 2016; Kjøltzow, Dobler, and Eide, 2018). Cold air is moved from the Arctic to the Norwegian coast where the ocean is warmed by the North Atlantic Current. The resulting temperature gradient gives rise to convection and subsequent electrification. As a result, there is a convective and electrically active belt along the coast of Norway during the winter, which is seen in the lightning climatology for winter in Kjøltzow, Dobler, and Eide, 2018. Winter lightning also differs from summer lightning storms in that the frequency of lightning strikes is lower and the polarity is often more positive (Michimoto, 2007).

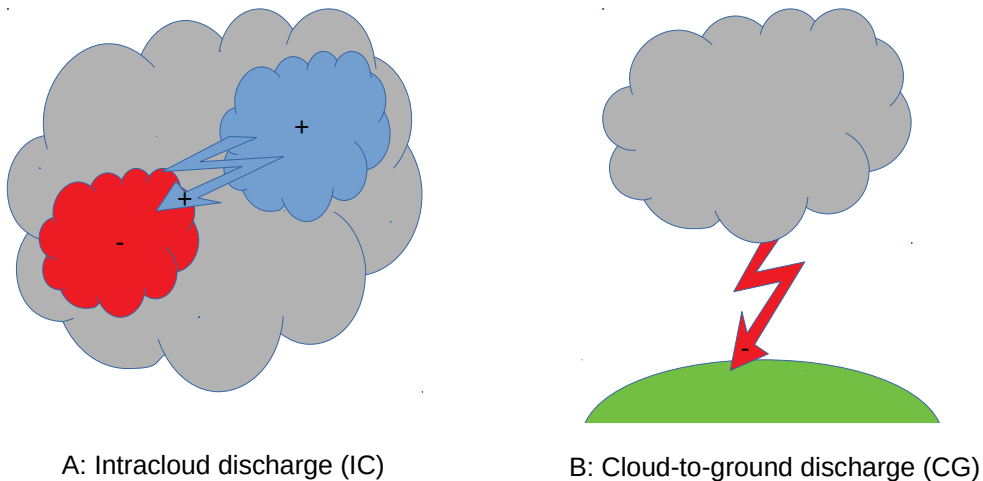


*Figure 2.1: Simple diagram illustrating the two main categories of lightning. A shows an Intracloud discharge (IC), this could be between different storm cells or between different charge areas of the same storm cell. B shows a Cloud-to-ground discharge (CG), the polarity is defined by the charge change of earth. Negative cloud-to-ground (-CG) is defined by increase of negative charge at ground, and so positive cloud-to-ground (+CG) is defined by decrease of negative charge (increase in positive) at ground*

## 2.4 Helicopter Triggered Lightning

A Helicopter Triggered Lightning is thought to be triggered by the helicopter's presence, such that the required electric field for this to happen can be much smaller than for natural lightning. This also means that a system that would create an HTL may be hard to identify, as natural lightning needs not precede the HTL.

Weather phenomena common to HTL-events are (from Lande, 1999):

- Outside air temperature (OAT) at current flight level near freezing point
- observed frozen precipitation, as snow, ice and graupel.
- clouds around or above the helicopter
- a cumulonimbus cloud within 5 nautical miles of the helicopter.

HTL is believed to be caused by the helicopter entering or coming close to an electrically charged part of a convective system. This may be caused by several different mechanisms:

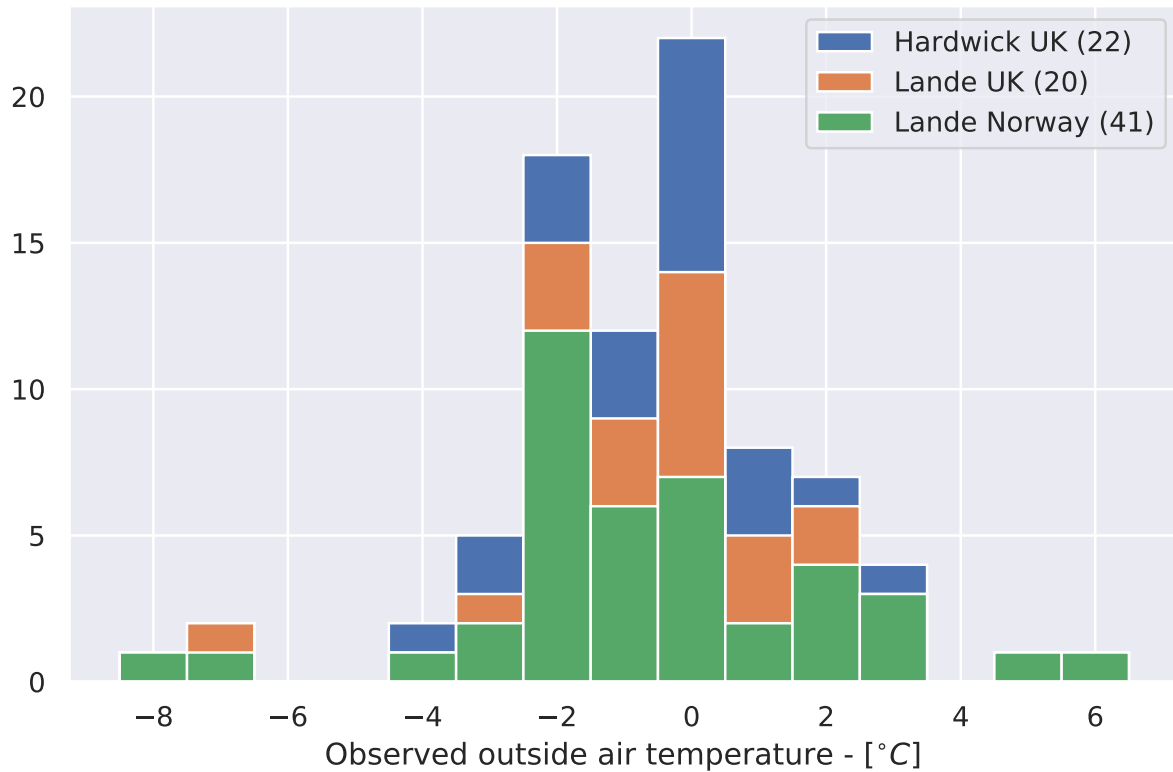


Figure 2.2: Outside air temperature (OAT) adapted from earlier HTL-studies, showing the 0 and -2 degree temperatures to be most represented in HTL-cases

The helicopter could be subject to a charge build-up during flight and then cause a discharge into the charged area of opposite polarity. However, given high enough charge density in the cloud, the charged area could also discharge into the helicopter *without* charge buildup in the helicopter. Alternatively, the helicopter could induce a CG by acting as part of the leader, see Figure 2.3.

During the 1960s and 1970s in the U.S. military, charge build-up on helicopters in-flight was studied to prevent static discharges seen when cargo helicopters were hooked up to equipment on the ground (Seibert, 1972). This phenomenon was found to be related to particles frictionally charging the helicopter blades. This charge was transported to the rest of the helicopter, since helicopters at the time were metallic. It was found that snow blowing through the rotors was a major factor in charging rate and accumulation, such that the maximum voltage measured between earth and helicopter was -200,000V when snow was blowing into the rotor (Seibert, 1962). This, in turn, led to the understanding that helicopters are negatively charged when flying in the North Sea (Wilkinson et al., 2013), such that a positive discharge is electrically favorable.



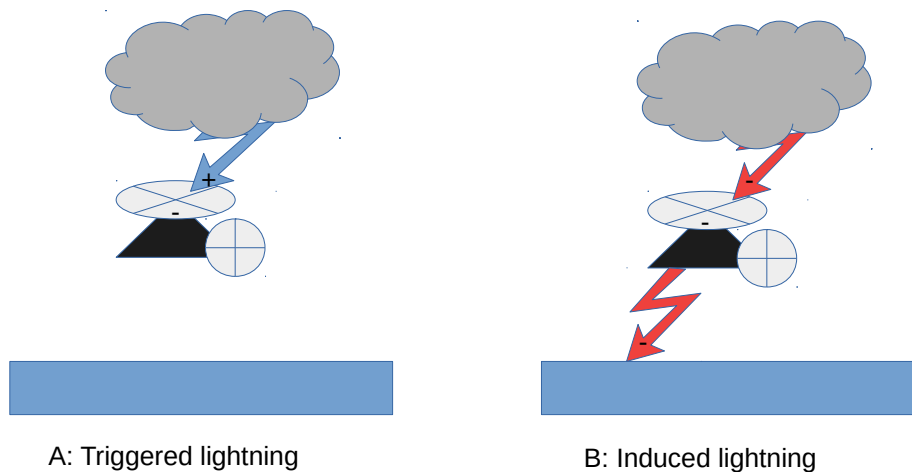


Figure 2.3: Illustration of different models for aircraft triggering. A shows the normal trigger situation, where the electrical discharge is grounded into the oppositely charged aircraft. B shows the situation where the aircraft is only acting as a pathway to the ground (Here ocean or land)

A positively charged discharge is believed to cause more damage to helicopters than their negatively charged counterparts, as the action integral (Joule work<sup>1</sup> integrated over time, assuming  $R = 1\Omega$ ) of a positive lightning is higher than that of a negative lightning (Hardwick, 1999). The discharges to helicopters seem to also more often be positive (Hardwick, 1999).

## 2.5 Fixed wing Triggered Lightning

As introduced in Chapter 1, a Fixed wing Triggered Lightning (FwTL) is a similar phenomenon to HTL: lightning triggered instead by the presence of an airplane or a rocket. The main difference between FwTL and HTL is that FwTL is not solely a winter phenomenon; it occurs during all seasons M. Uman and V. Rakov, 2003. Presumably, this is because planes fly higher and in a larger range of altitudes than helicopters: In summer, convective clouds can reach the tropopause, causing the electrical parts of the clouds to be spread further up, whilst in winter, the convection is not as deep, and the electrical parts of the clouds are closer

<sup>1</sup>Any conductor has heat work ( $J$ ) based on the resistance ( $R$ ) and the current ( $I$ ) through the conductor:  
 $J = I^2R$

to the surface (e.g. M. Uman and V. Rakov, 2003; Michimoto, 2007).

## 2.6 Helicopter Trigger Index

As stated in Chapter 1, operational forecasting of HTL is relatively new. In Norway, the Norwegian Meteorological Institute began forecasting the risk of HTL, Helicopter Trigger Index (HTI), in 2016. The theory behind the forecast is based on findings by Hardwick, 1999 and Wilkinson et al., 2013, and HTI is computed from four sub-indices, which are based on the following meteorological factors:

- **Vertical wind speed** in the altitude that helicopters generally fly in.
  - Computed from the maximum vertical wind speed within the 7 nearest grid cells in the forecasting model.
  - Positive (upward) vertical wind gives a non-zero value, and negative (downward) vertical wind gives 0 value.
  - Figure 2.4a shows the conversion between vertical velocity in  $m/s$  and this sub-index.
- **Temperature** at the altitude that helicopters generally fly in.
  - Temperatures in the  $[0, -6]^{\circ}C$  range gives non-zero value.
  - 0 for temperatures outside this range
  - Figure 2.4b shows the conversion between temperature in  $^{\circ}C$  and this sub-index.
- **Total precipitation** during the last hour.
  - Computed from the maximum precipitation within the 7 nearest grid cells in the forecasting model.
  - Linear from  $0 \frac{mm}{hr}$  with 0 value to full value at  $0.75 \frac{mm}{hr}$  precipitation intensity.
  - Figure 2.4c shows the conversion between precipitation intensity in  $mm/hr$  and this sub-index.
  - An error in the system producing the HTI was found to be using the Accumulated total precipitation, and is described in 2.6.1
- **Low clouds** in the surrounding area.
  - Computed as the difference between the maximum and minimum cloud cover within the 7 nearest grid cells in the forecasting model.
  - Full cloud cover gives value 0, to exclude stratiform cloud systems and fog. No clouds also gives value 0.

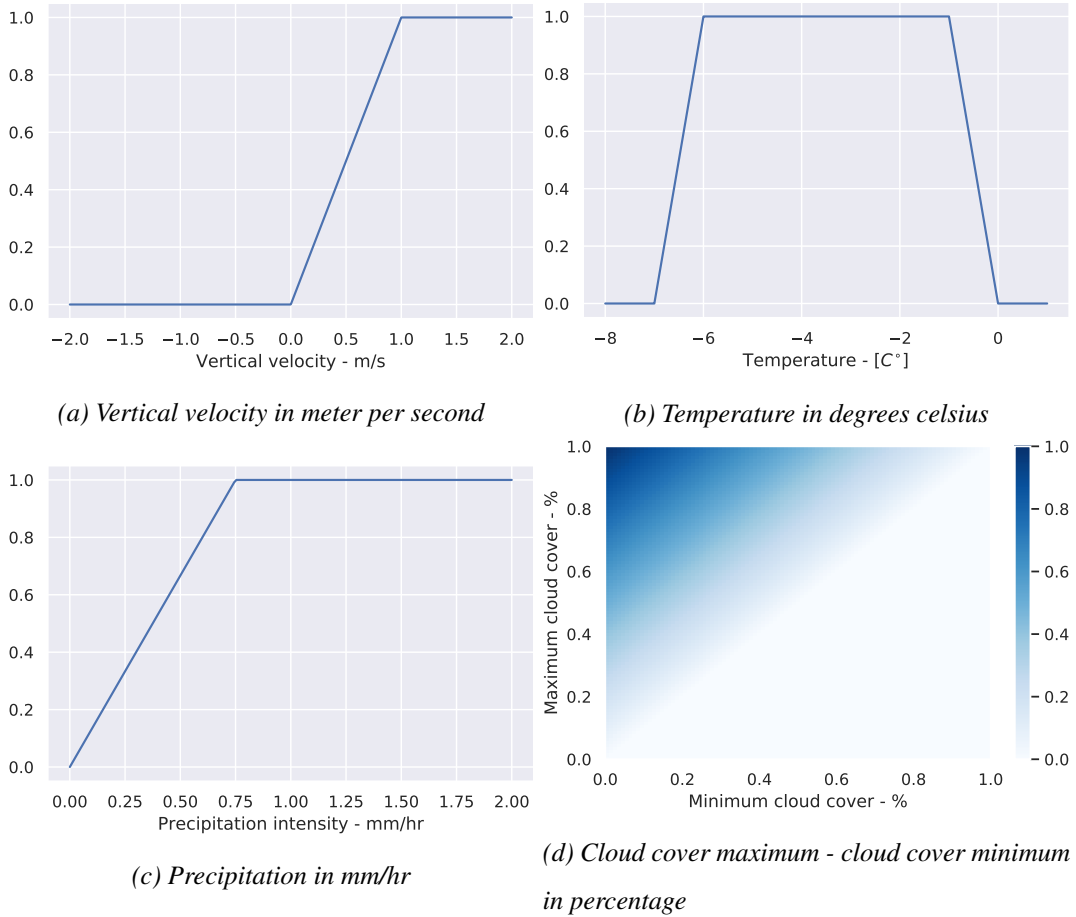


Figure 2.4: Sub-index value for different input for the four parameters used in the calculation of HTI

- Figure 2.4d shows the conversion between minimum and maximum cloud cover and this sub-index.

To prevent under-forecasting due to convection being placed incorrectly in the forecast system, the vertical velocity, cloud and precipitation parameters use a neighbourhood approach to capture the spatial variation. The total HTI is the sum of these four sub-indices,

$$HTI = \frac{\text{Vertical Wind}}{4} + \frac{\text{Temperature}}{4} + \frac{\text{Precipitation}}{4} + \frac{\text{Cloud}}{4}$$

equally weighted, such that HTI is valued in the range  $[0, 1]$ . The index is categorized in four different classes of severity, from no danger (White) to very high risk (Red). See figure 2.5 for example and A.10 for procedures.

- White:  $HTI < 0.73$
- Yellow:  $0.73 \leq HTI < 0.90$
- Orange:  $0.90 \leq HTI < 0.99$

- Red:  $0.99 \leq HTI$

The severity categories are based on discussion with the main offshore helicopter operators in Norway (Bristow and CHC), and are changed if deemed necessary after the yearly evaluation of the season. HTI is not based on a regression analysis, but rather a subjective review of the earlier cases of incidents.

### **2.6.1 Precipitation error in HTI**

When trying to recreate the HTI-functions during the work, it became apparent that the operational forecast had been wrongly using the accumulated precipitation and not the intended hourly precipitation. This shifted some of the investigation into whether this erroneous use of the accumulated precipitation had led to any significant over-forecasting of HTL. The result of this would be limiting helicopter flights when there had been precipitation forecast earlier. Thus, any precipitation would lead to the precipitation sub-index to take the value one (1) (the maximum) for the rest of the forecast. For example, precipitation during the first hour of a forecast could wrongly overestimate the HTI of the following 17 hours of forecast made available to the flight planner.

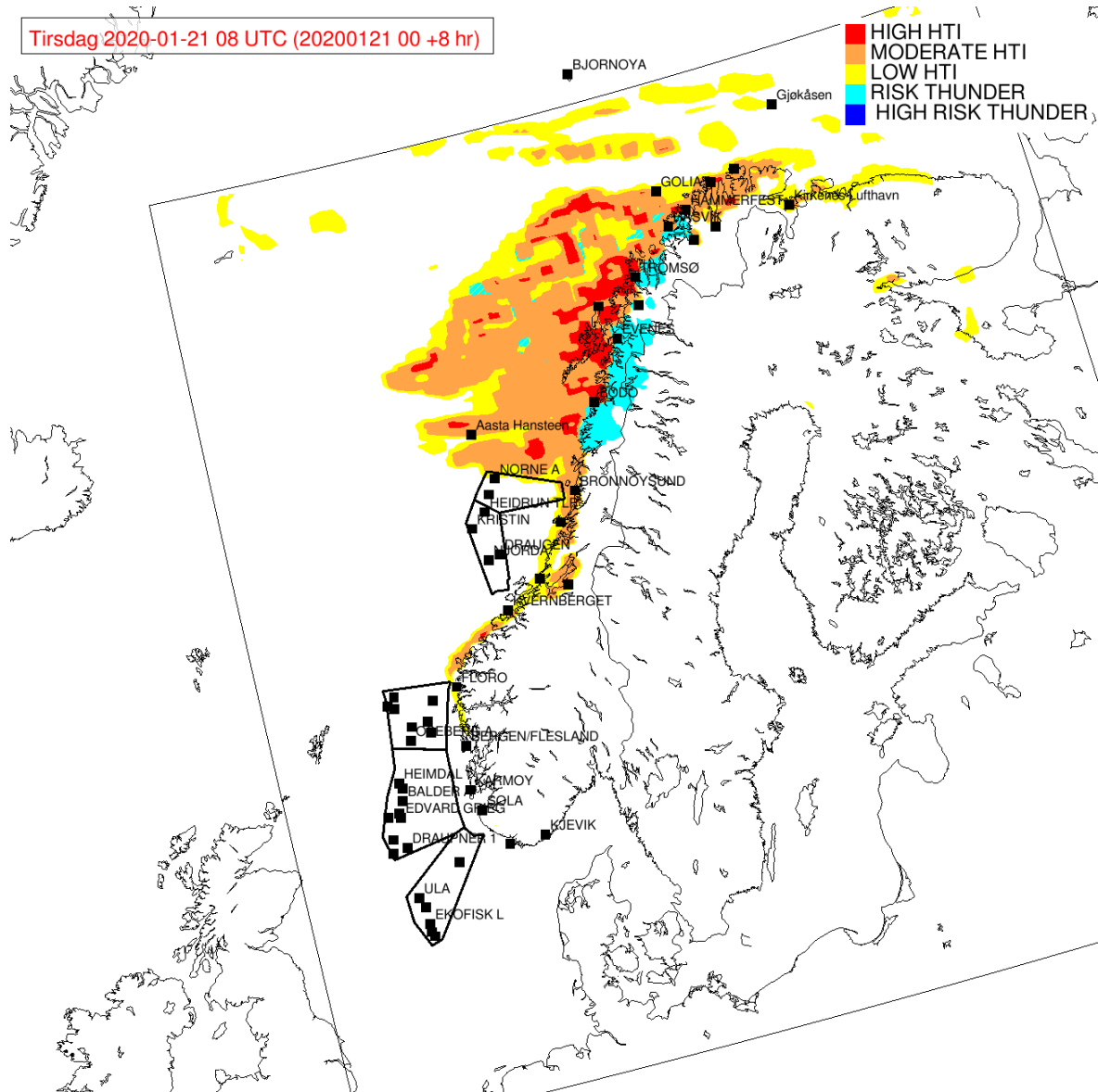


Figure 2.5: Screenshot from <https://www.ippc.no> for 21. of January 2020, showing the HTI-forecast with 8 hour lead-time after midnight. The blue thunder-cells show another forecast-product from MET, forecasting risk for natural lightning. A plane was hit by lightning, and was therefore diverted from flying into Bodø during this forecasts valid time.



## 3 Methods

This chapter briefly describes the model data used herein as basis for the atmospheric state at the time of lightning related incidents. It also describes observational data (meteorological observations and incident reports) used to investigate weather conditions during HTL incidents. Further, the different methods of data processing is described. Lastly, some limitations are discussed.

### 3.1 Models

It is important to distinguish between the two model types used in this thesis. This section intends to explain both the general idea behind the model types, and the specifics pertaining to the chosen models.

#### 3.1.1 Numerical Weather Prediction - model

A Numerical weather prediction (NWP)-model uses observational data as input to create an analysis for the current atmospheric state. This is done such that the model is run with the best estimate of the atmosphere. When the model then runs it advances in time, with a given timestep. This advance is done by solving the governing equations to calculate the next state of the atmosphere. This state is then recorded at fixed intervals and this predicted/forecasted state is what constitutes a weather forecast. Operational NWP-models are often updated when model upgrades are ready, so models for different time periods can be using different physics schemes. Modern NWP-models also utilize perturbed ensemble-members. This is done by having a control run use the original observational data, and then making small (inside of the observational uncertainty range) changes or perturbations to the initial state. This could also include changes to the model itself (e.g. Toth and Kalnay, 1993). Each run is then a member in the whole ensemble, and the ensemble as a whole is meant to represent a range of possible outcomes from the observed starting state.

#### MEPS

The operational MetCoOp ensemble prediction system (MEPS)<sup>1</sup> model uses a timestep of 75s, a horizontal grid with a 2.5x2.5km resolution, with 65-vertical model levels in the

---

<sup>1</sup>Note that in February 2020, both the format and frequency of model runs for MetCoOp ensemble prediction system (MEPS) was changed considerably, operational here refers to the model-runs from 2016-2019

HARMONIE-AROME system (Bengtsson et al., 2017). The data is recorded at *1hr*-intervals and output at both pressure and the hybrid sigma levels from the model. Archived data for this model-setup is available for the period 2016 to 2019 at [thredds.met.no](https://thredds.met.no). MEPS became available in November 2016, and hence can only provide atmospheric conditions for cases that have occurred since then.

### 3.1.2 Reanalysis - model

A reanalysis differs from an operational NWP-model in that it uses a fixed version of an NWP-model on historical weather observations. This is done to create the best possible historical weather data, by turning point and field observations into a complete gridded archive of historical weather. Reanalysis models may also be run with pertubated ensembles, to capture variation between the times when observational data is considered.

#### ERA5

The ECMWF atmospheric reanalysis (ERA5) data set is created by the European Centre for Medium-Range Weather Forecasts (ECMWF) and provides hourly data, in 31x31km grids, with 137 vertical model-levels. The data ranges from 1979 to and including 2019 (At the completion of this thesis. ERA5 is continually updated). The observational data is assimilated in 12-hour windows (Hersbach et al., 2018). This thesis utilizes the ERA5 data set to create a set of climatologies and case-based atmospheric conditions, using the data reported on pressure levels.

## 3.2 Data

### 3.2.1 Incidents from Avinor

For the purpose of this thesis, the author received a data set from Avinor. This data included all reports on helicopter and plane incidents reported to Avinor pertaining to lightning. To utilize this data set, cases where there was observed lightning in the area and not striking the aircraft, has been filtered out to prevent identifying "normal" lightning. Further a filter has been applied to the geographical positioning of this data set, such that all incidents related to either take-off or landing are moved to the position of the respective airport. No attempt has been made to identify the position of aircraft en-route (between two locations), as this was not available in the data set. Cases without exact position recorded are therefore only included in analysis of larger geographical zones herein. These zones are defined in Figure B.1 in Appendix B. The Avinor data set covers the years 2008 to late 2018, and as such



	Total cases	Height info	Position	Reported temp. (OAT)	After November 2016
Helicopters	40	37	24	12	19
Fixed-wing	256	217	256	1	57
Total	296	254	280	13	76

*Table 3.1: Data available for each case in the Avinor-dataset. Note that there is one helicopter case where height is not known, but position is.*

METAR-code	Description
CB	Cumulonimbus cloud
TCU	Towering Cumulus cloud
RA	Rain
SN	Snow
GS	Hail
GR	Graupel
SH	Showers
VCSH	Showers in vicinity
FEW	Few clouds (1-2/8)
SCT	Scattered clouds (3-4/8)
BKN	Broken clouds (5-7/8)
OVC	Overcast (8/8)

*Table 3.2: METAR-codes for reporting weather phenomena. The last four categories includes a numerical value for how much of the cloud is covered by clouds, OVC refers to total cloud cover, FEW refers to one to two eights of sky is cloud*

covers a larger period than MEPS-archives, which is why ERA5 was included. The data set has been summarized in Table 3.1. The author has only been authorized to share statistics and analysis done on the data set, not the data set itself.

### 3.2.2 Meteorological aerodrome report

Meteorological aerodrome report (METAR) is a report given every half hour at airports throughout the world, to monitor whether the weather allows flying. This is a subjective report of the current weather generated by trained personnel or in some cases automated by instruments. The METAR report is a listing of relevant meteorological phenomena, but will always include certain parameters. In this thesis the categories listed in Table 3.2 are used, due to their relation to convective clouds, which in earlier studies has been related to triggered lightning incidents.

## 3.3 Composite plots

In the meteorological field it is common to use composite plots to investigate the atmospheric situation related to a type of incident. Given a data set of certain parameters related to the specific type of incident, the composite plots consist of a mean and a standard deviation over these parameters in the data set. This is done to visualize the commonalities in the set of cases and the differences between them, to identify what conditions are generally present for the incident type.

In this thesis, composite plots are produced to study atmospheric conditions during triggered lightning incidents. Using the location and temporal information from HTL and FwTL incidents in the Avinor data set (see Section 3.2.1), in combination with ERA5 data (see Section 3.1.2), atmospheric conditions are reproduced for the incidents. After being grouped into different geographical regions (to study to what degree incidents in the same area might occur in similar atmospheric conditions), composite plots are computed.

Where the standard deviation is low, the mean is significant for the set of cases. If the standard deviation is high, it may either be due to insignificance or local spatial variation in the data set.

## 3.4 Decomposition of HTI

To investigate the performance of the Helicopter Trigger Index, it is important to study the current index during all the registered incidents of triggered lightning. Since HTI is the sum of sub-indices (see Section 2.6), the effects of the sub-indices are studied. During any triggered lightning incident where the forecasted HTI is lower than Red, such a decomposition might suggest which of the sub-indices is failing. Any commonalities in sub-indices that under-perform might suggest improvements to HTI.

## 3.5 Interpolation

Since the data used in this thesis is sparsely populated both temporally and spatially, it is necessary to interpolate. To calculate both the vertical velocity and the temperature interpolation is used to get the velocity and temperature representative for a specific height. This is done by calculating a linear vertical change rate and then multiplying this change with the difference in height. The temperature for a given height  $H$  between a higher and lower level

with temperatures  $T$  and height  $Z$  is then found by:

$$T_H = T_{lower} + \frac{T_{higher} - T_{lower}}{Z_{higher} - Z_{lower}}(H - Z_{lower}) = T_0 + \frac{\Delta T}{\Delta Z}\Delta H$$

The same procedure is applied on the vertical velocity  $W$ :

$$W_H = W_0 + \frac{\Delta W}{\Delta Z}\Delta H$$

See Section 3.6.2 for limitations with the current interpolation scheme.

## 3.6 Model limitations

The usage of forecasting and reanalysis model data will always bring with it uncertainties, since there is always both spatial and temporal uncertainty in models. The resulting limitations in analysis of ERA5 and MEPS are discussed herein.

### 3.6.1 Temporal uncertainty

Temporal uncertainties arise from the fact that model data is output at hourly time steps, meaning that processes which happen on shorter timescales cannot be captured accurately. In this thesis, only nearest hour has been used when collocating model data to incidents and observational data. No other effort has been made to reduce the temporal uncertainty.

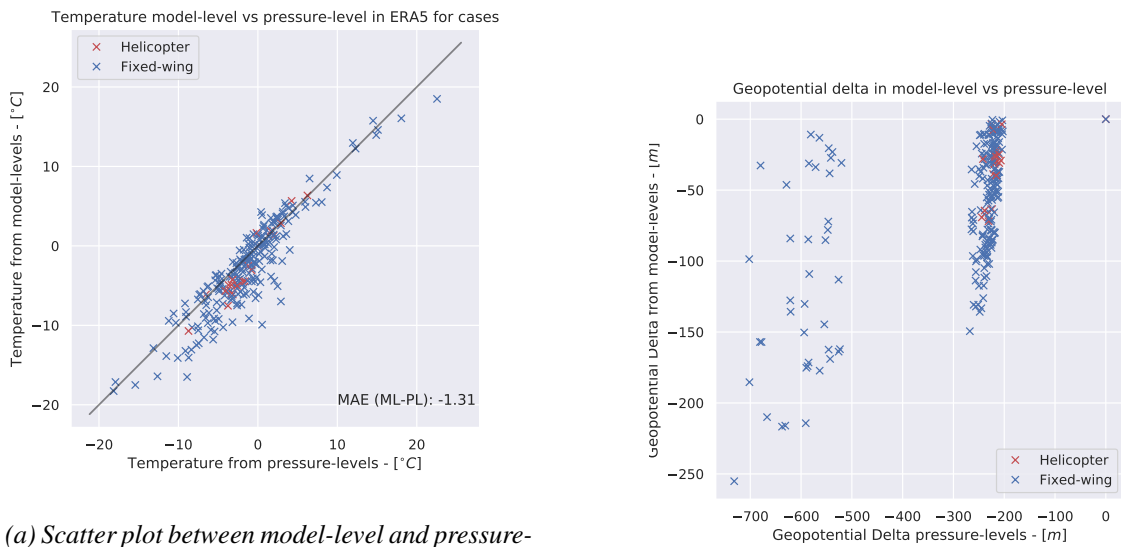
### 3.6.2 Pressure level vs Model level interpolation

As mentioned in the Section 3.5, the model data is sparsely populated, and this will in turn introduce an uncertainty. To prevent the vertical uncertainty a interpolation was applied (motivated also by the fact that interpolation is used in the operational forecast). The MAD is a statistical tool used to determine systematic difference between two different dataset containing  $n$  variables  $x$  and  $y$ . It is calculated by:

$$\text{MAD} = \frac{\sum_{i=1}^n |y_i - x_i|}{n}$$

Figure 3.1 shows the difference between model level and pressure level interpolation in ERA5. Since both are model products, it is not certain which is the "correct" situation, such that the MAD only shows the difference between the data set, and not a bias for one compared to the other. Figure 3.2 shows the difference of ERA5 and MEPS temperatures found from pressure level interpolation to case height for triggered lightning incidents. The substantial difference in temperature arises from ERA5 having a much finer pressure level output (850hPa to 1000hPa was represented for each 25hPa interval), whilst MEPS have a much coarser level output: only 1000hPa, 925 and 850hPa was available at the same 850hPa to 1000hPa interval. The 850hPa to 1000hPa range should contain all HTL-incidents.

### 3.6. MODEL LIMITATIONS



(a) Scatter plot between model-level and pressure-level interpolation of temperature from ERA5, also printed on the figure: Mean Absolute Difference (MAD), showing model-level interpolation averagely colder than pressure level interpolation with 1.31° Celsius.

(b) Scatter plot between model level and pressure level interpolation of geopotential height from ERA5.

Figure 3.1: Difference between model level and pressure level interpolations for a) Temperature and b) geopotential height. The temperature is found by geopotential height as discussed in Section 3.5, such that these variables are not independent.

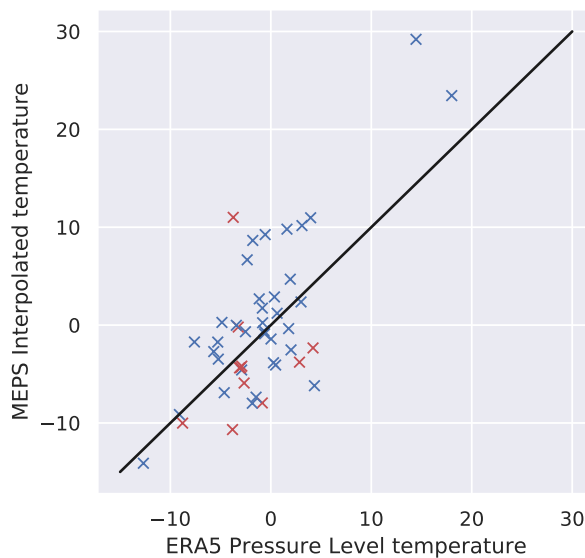


Figure 3.2: Difference of ERA5 and MEPS temperatures using pressure level interpolation to case height.

### 3.6.3 Loss in data due to archiving

Due to the Meteorological Institute reducing their available archived model data, the vertical velocity parameter was not available for cases before October 2018. To perform the decomposition analysis, the vertical velocity sub-index was determined from its relation to HTI:

$$\frac{\text{Vertical Wind}}{4} = \text{HTI} - \left( \frac{\text{Temperature}}{4} + \frac{\text{Precipitation}}{4} + \frac{\text{Cloud}}{4} \right)$$

Thus the HTI was needed to calculate the vertical velocity, and as such the cases where HTI was set to zero by the land-sea mask, the vertical velocity index was not retrievable.



## 4 Results and discussion

### 4.1 Analysis of Avinor triggered lightning data set

As discussed in Chapter 2, there exists a body of research showing that the  $0^{\circ}\text{C}$  isotherm in a cloud is related to winter- and Helicopter Triggered Lightning. Figure 4.1 shows that the Avinor data set has the same seasonal variation as these earlier studies, except for the additional case in May. This is presumably due to the Norwegian climate being generally colder than the British, which is where most of the earlier cases were from. Additionally, Figure 4.3 shows an increase in HTL cases after the introduction of the operational forecast, with a rate of 2 incidents per year before the forecast was introduced, to 5.5 incidents per year afterwards. Looking at the source data set, this seems to be more of a increase in reports from helicopter operators than an actual failing of the HTI. This is due to an increase in reports about incidents with no damage.

In contrast to the earlier research, the temperature found from ERA5 in Figure 4.2 shows that the peak is situated around  $-3^{\circ}\text{C}$  and not the  $0^{\circ}\text{C}$  isotherm. This can either be attributed to a systematic error in pressure level interpolation (see Section 3.5), or due to operational

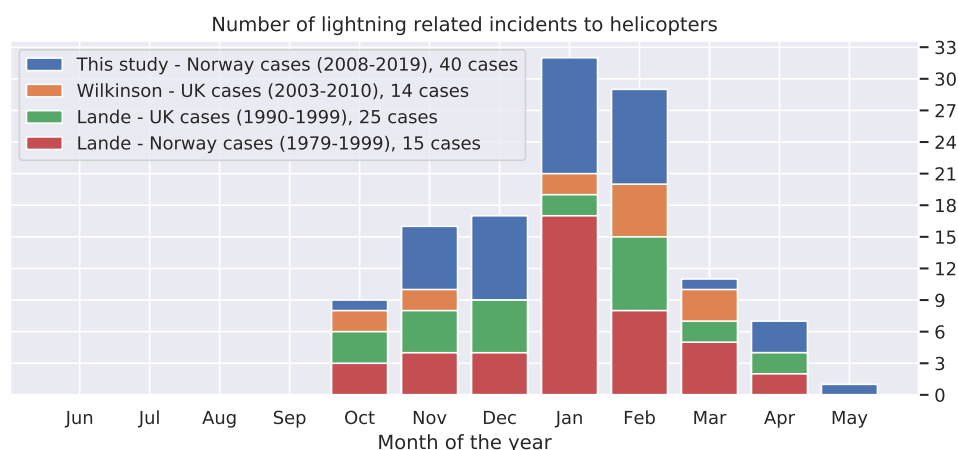


Figure 4.1: Seasonal variation of helicopter cases, showing no cases in June to September. Same as Figure 1.1, with cases looked at in this study added to it. Older data is produced from Lande, 1999 and Wilkinson et al., 2013. Legend notes time-periods and amount of cases in each study.

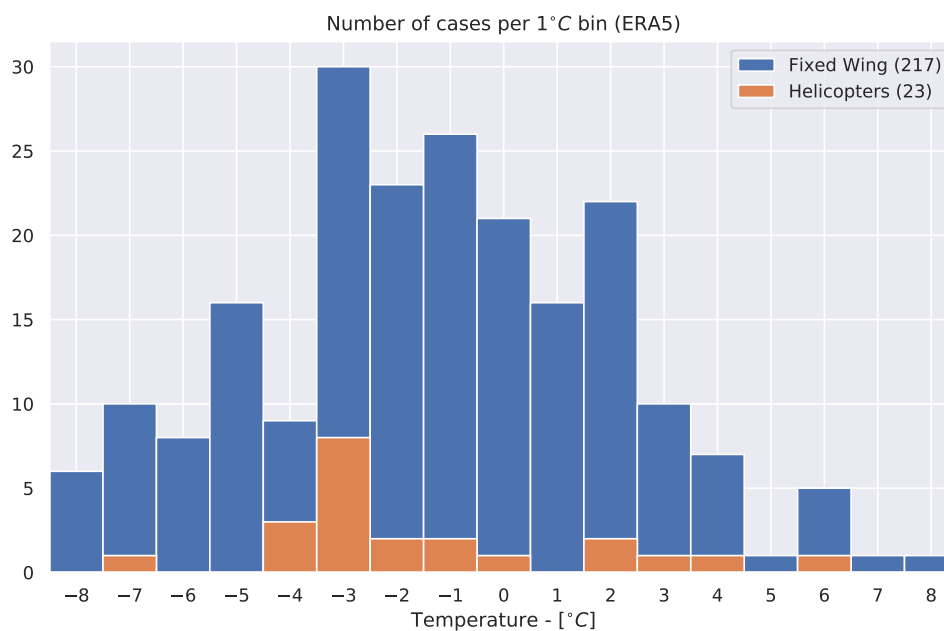


Figure 4.2: Temperature in fixed-wing and helicopter cases (interpolated from ERA5 pressure levels)

procedures implemented due to Lande, 1999, which advises avoidance of the  $0^{\circ}\text{C}$  isotherm when HTL is forecast or when flying inside of a cloud. Taking into account the FwTL temperature in the same figure, there seems to be a  $-1^{\circ}\text{C}$  shift from  $0^{\circ}\text{C}$  since the peaks are at  $-1^{\circ}\text{C}$  and  $-3^{\circ}\text{C}$  compared to Figure 2.2. This also supports the previous statement about the effect of avoiding the  $0^{\circ}\text{C}$  isotherm, as this is not a procedure followed by pilots flying fixed wing aircraft.

Figure 4.4 shows the HTL incidents divided by the zones shown in Figure B.1. It should be noted that there are no cases at Gardermoen, and only one case off the coast of Denmark in the Southern coast zone. The April peak is primarily contributed to by the North coast zone, which can be explained by the fact that the sea is still relatively warmer than the atmosphere during this time compared to the coast further south. This therefore supports earlier work in which it was proposed that cold air over warmer oceans caused convective systems to appear and be electrified.

Figure 4.5a shows the same picture that HTL is a winter phenomenon and supports the claim in Section 2.5 that FwTL is an all-year phenomenon. The august peak in FwTL can be explained by August being the month with the highest lightning activity in Norway. July also



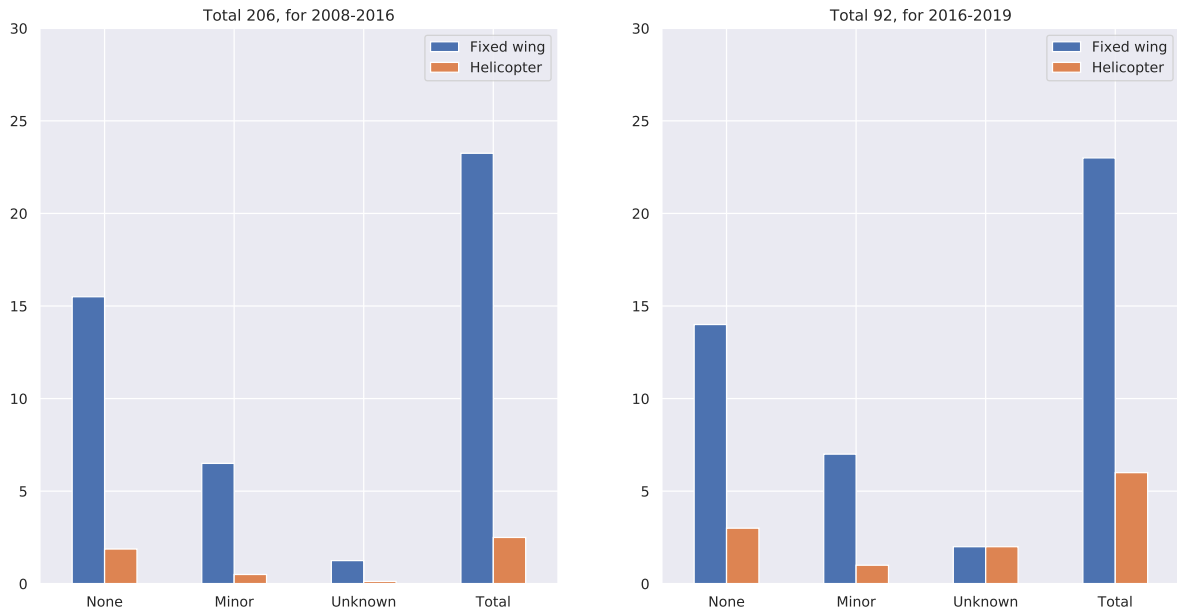


Figure 4.3: Cases per year from the Avinor data set, delineated between cases before operational forecast was in place in the left figure, and after operational forecast was used in the right figure.

has some lightning activity, but commercial air travel is reduced compared to August.

Figure 4.5b shows that there is a geographical variation in cases, namely southern coast and Gardermoen primarily have cases during April-October, whereas the north, west and northwest are more represented during October-April. This shows a similar picture to that in Køltzow, Dobler, and Eide, 2018: The Norwegian lightning climatology is primarily coastal in nature for winter lightning, and primarily inland for summer lightning.

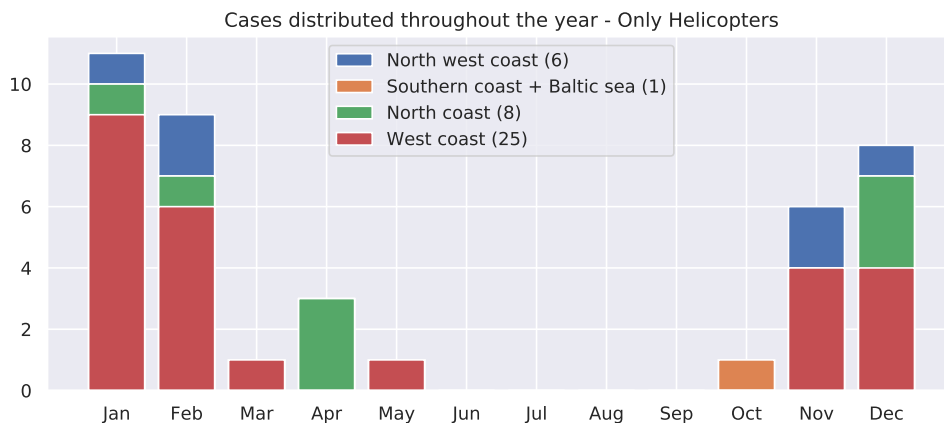
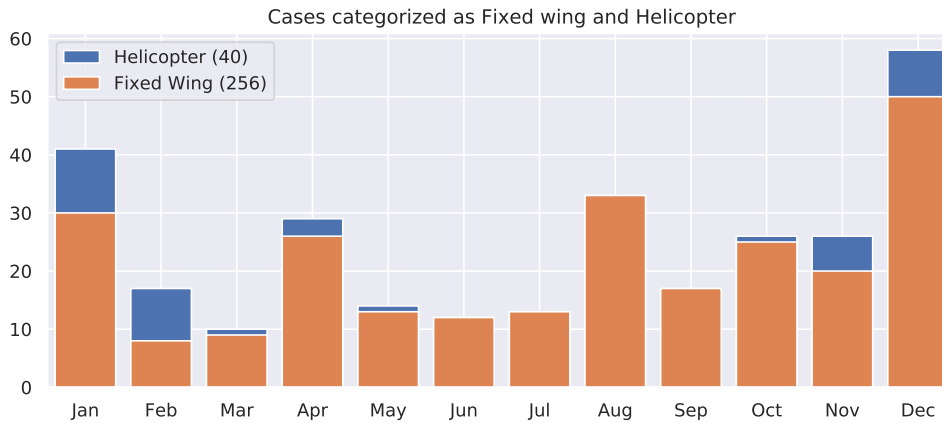
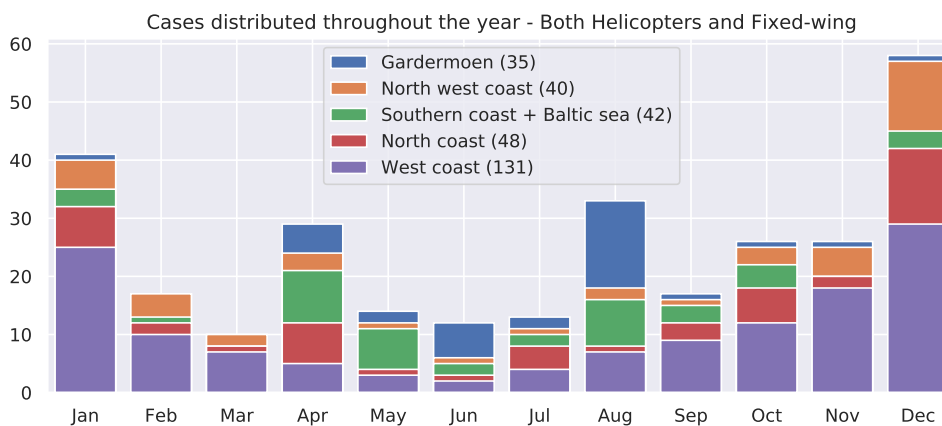


Figure 4.4: Zonal division of helicopter cases



(a) Yearly distribution of helicopter and fixed wing cases



(b) Zonal division of helicopter and fixed wing cases, see Figure 4.5a for categorical distribution

## 4.2 Meteorological phenomena related to triggered lightning

### 4.2.1 METAR observations

Figure 4.6 shows the meteorological phenomena reported in the METAR report during triggered lightning incidents (both HTL and FwTL). The helicopter cases show a high frequency (above 50 %) for scattered, few and broken clouds, but zero of the cases had overcast conditions. Also found were showers in 20 % of the cases, and rain and/or snow was found in more than 20 % of the cases. Only 20 % of the cases had a report of cumulonimbus clouds. For the fixed wing, the cumulonimbus frequency is much higher (60 %), and rain was in 40 % of the cases and snow in less than 5 %. Showers were also often reported (60 %). The fact that snow was less often reported for fixed wing compared to helicopter cases may

be due to it being an all-year phenomenon such that snow was not observed at the ground during summer events. This, in turn, supports both Lande, 1999 in that cumulonimbus was not *always* observed during triggered lightning incidents, and the choice to include maximum cloud cover minus minimum cloud cover since almost none of the cases show overcast conditions.

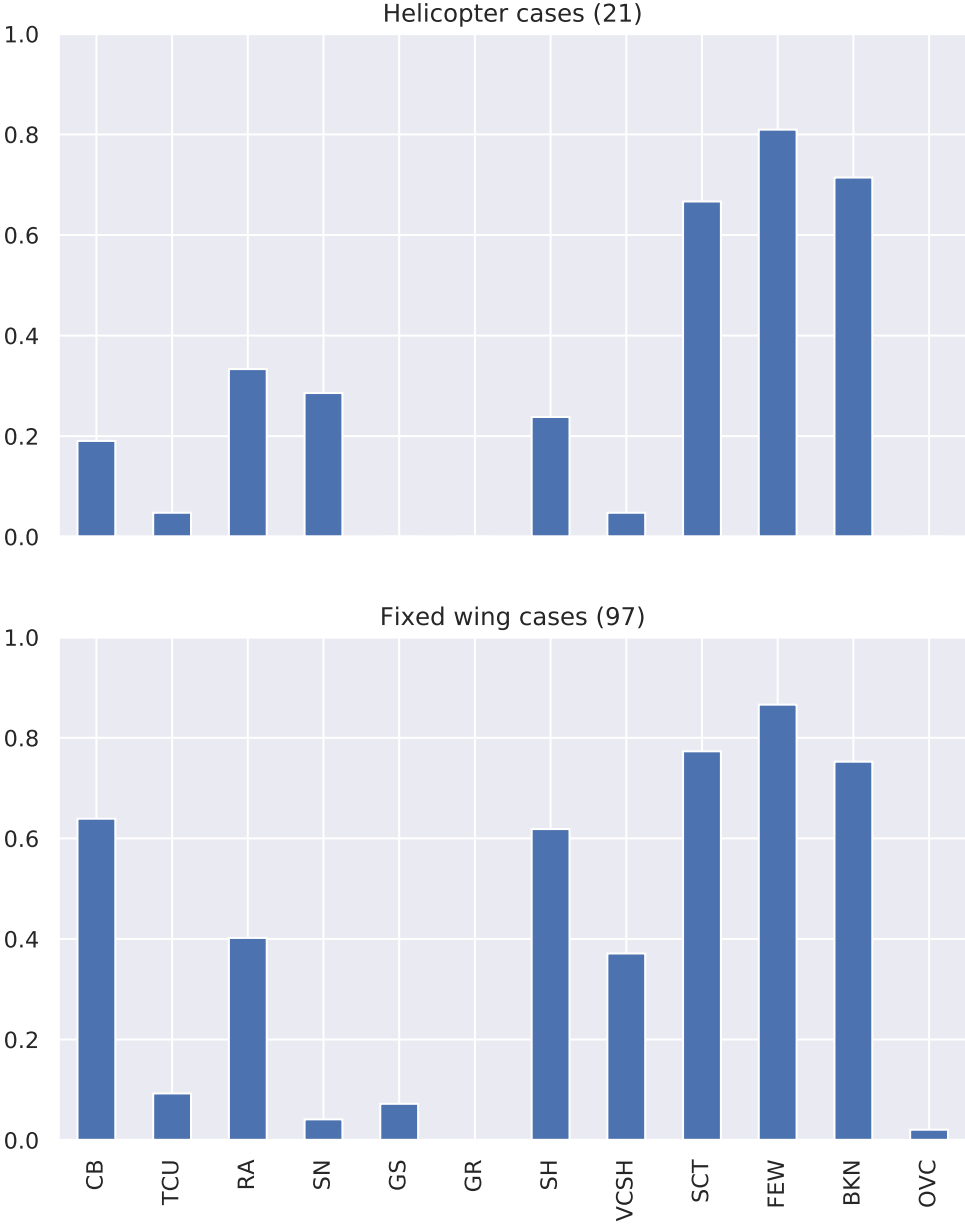


Figure 4.6: Frequency of different categories of METAR-phenomenon for Helicopter and Fixed wing cases, included are only cases where airport had a METAR-report that was taken by a non-automatic system. Note that SH also include VCSH

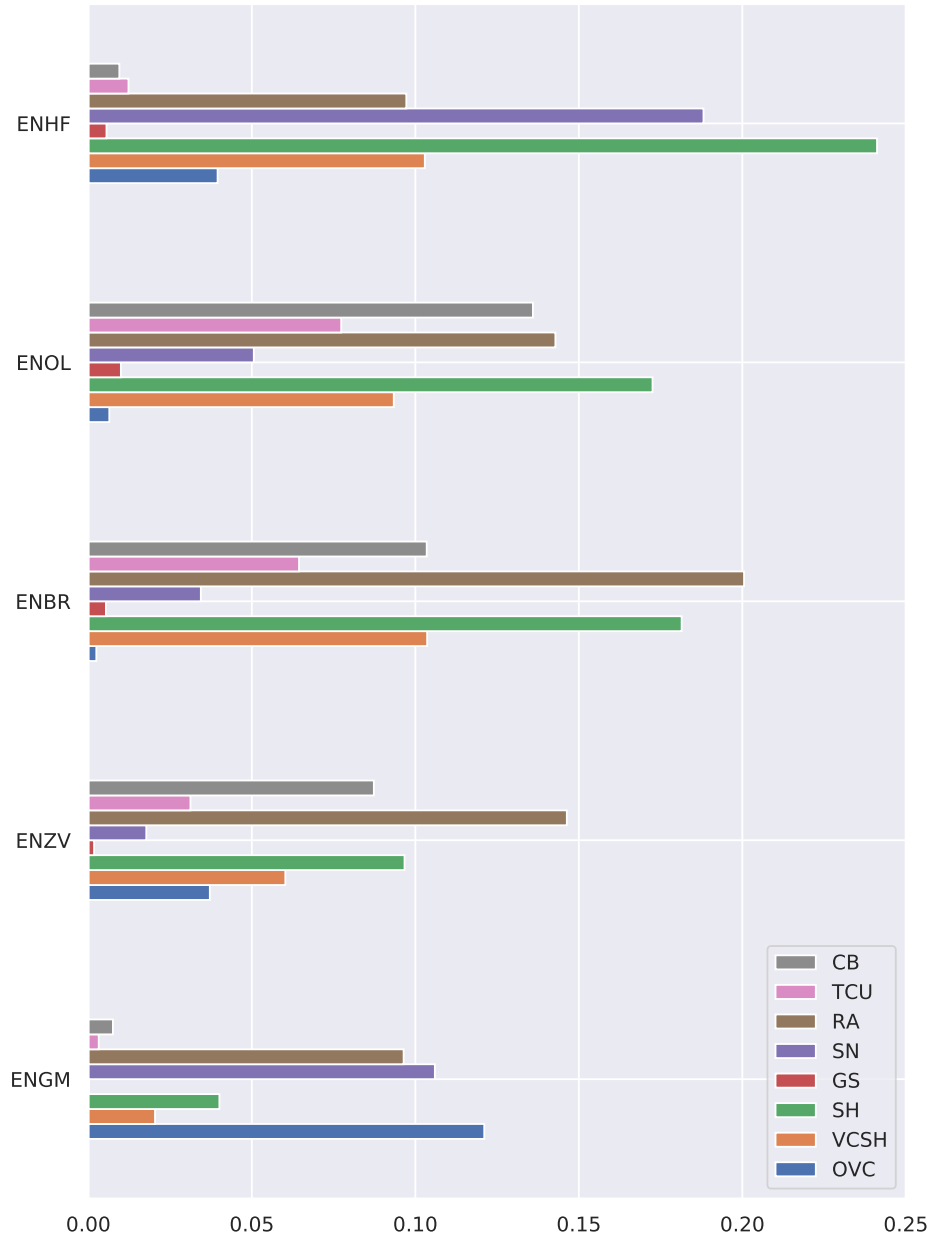


Figure 4.7: Percentage of METAR-reports involving at least one of the meteorological phenomena at Hammerfest, Ørlandet, Flesland, Sola, and Gardermoen airports. Selection is based on geographical variation and representation.

To investigate the parameters used in the operational HTI forecast, composites have been created for the cases from the Avinor data set. The parameters studied are temperature, vertical velocity, precipitation and cloud cover. Cloud cover did not show any clear signal due to ERA5 horizontal scale, and therefore was moved to Appendix A. Also studied is the general circulation during these cases, by looking at the composite of the mean sea level pressure.

### 4.2.2 Temperature during triggered lightning events

Shown in Figure 4.8 are temperature composites divided into the geographical zones described in Appendix B. The figure reveals that for the different geographic zones, the average temperature in the composites are around  $-3$  to  $0^{\circ}\text{C}$ . This is in accordance with previous findings that HTL happens at temperatures right below or at  $0^{\circ}\text{C}$ . One also sees that grouping of the cases leads to a reduction in the standard deviation along each zone's coast, except for the North zone. This hints to that these temperatures are closely related, but North zone should ideally be divided into finer zones. (This would, however, be less robust due to the North zone only containing 40 cases.)

Figure 4.9 shows that the temperatures at Flesland and Sola are, as expected, around  $0$  to  $-1^{\circ}\text{C}$ , and here the variation in temperature is much lower as seen in the respective standard deviation plots. The standard deviation is lowest in Flesland, but this is to be expected, since there are double the amount of cases at Flesland than Sola. Looking, though, at Figure 4.9c, one sees that Gardermoen airport has a much warmer situation at around  $+2^{\circ}\text{C}$ . Here, the standard deviation also is higher. This coincides with the variation shown in Figure 4.2.

### 4.2.3 Typical pressure pattern during triggered lightning events

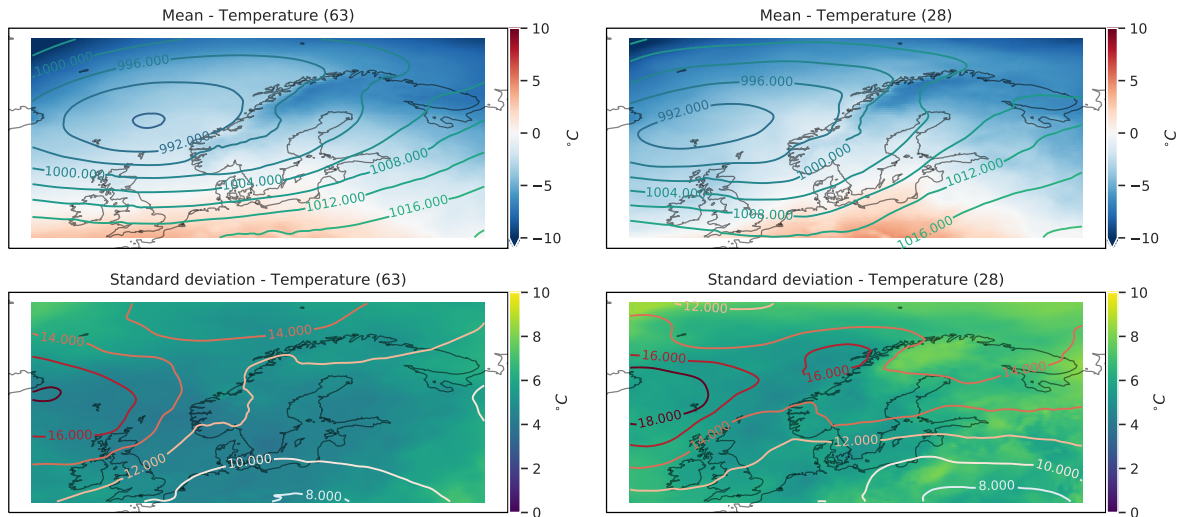
Figure 4.8 contains, in addition to temperature, composites of pressure during triggered lightning events. The general circulation from these pressure systems seems to tend toward geostrophic wind directed toward the coast. Notable exception is the South zone, which does not have a clear low pressure system in the ocean, but the standard deviation hints to a lot of variation over the ocean. The geostrophic winds for the remaining zones also would be coming from colder areas, i.e. Iceland and the Arctic. This would lead to cold air being blown over the relatively warm North Atlantic Current, as discussed in Section 2.3.1, as a precursor for convection and lightning activity. The pressure in Figure 4.9 shows the same picture for both Flesland and Sola airports, being dominated by low pressure systems situated in the

Norwegian Sea, such that the geostrophic wind would be directed inland toward the airports. The convection observed here may be a result of topography and surface roughness changing when moving from ocean to land. Since the land does not dissipate the kinetic energy in form of waves, the energy leads to more turbulence in the air, causing local convection. This suggests that wind incident on land is present in most cases of triggered lightning events at the coast of Norway.

However, Gardermoen being located inland does not see this roughness effect. This suggests that incidents at Gardermoen are instead related to local convective systems seen in the summertime. This explains why Gardermoen airport's pressure situation is "normal" during triggered lightning events, since the incidents are related to local convective systems, rather than bigger circulation causing local convection. The standard deviation shows the same picture in that the pressure does not have a large standard deviation.

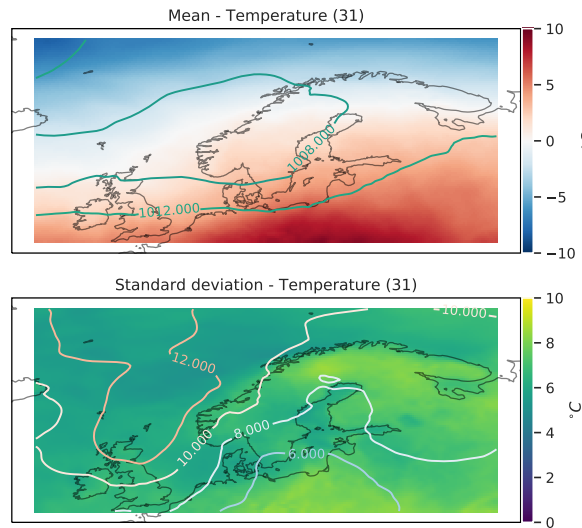






(a) Temperature for cases at Flesland airport.

(b) Temperature for cases at Sola airport.



(c) Temperature for cases in Gardermoen zone.

Figure 4.9: Same as Figure 4.8, but for only the biggest airports.

#### 4.2.4 Vertical velocity during triggered lightning events

Figure 4.10 shows vertical velocity composites for the different geographic zones. It should be noted that the color bar is inverted, such that red is negative and blue is positive. This is done due to the units being Pa/s, so that negative values infer upward velocity and positive downward velocity. One can see a clear trend among the coastal zones (north, northwest and west) that there is upward vertical velocity related to the cases. There is also a somewhat high standard deviation in these same zones, but this could be related to *placing* of the upward velocity systems in the model. Looking at Figure 4.11, one sees the same for both Flesland and Sola: A clear vertical velocity in the composite, but some higher standard deviation in the Sola case. (Again, presumably because of the lower number of cases.) There is a

## 4.2. METEOROLOGICAL PHENOMENA RELATED TO TRIGGERED LIGHTNING

very weak vertical velocity for the Gardermoen case. This can be explained by Gardermoen predominantly being subject to summer lightning, which is due to local convective areas and may not be correctly resolved in the coarse horizontal grid of ERA5.

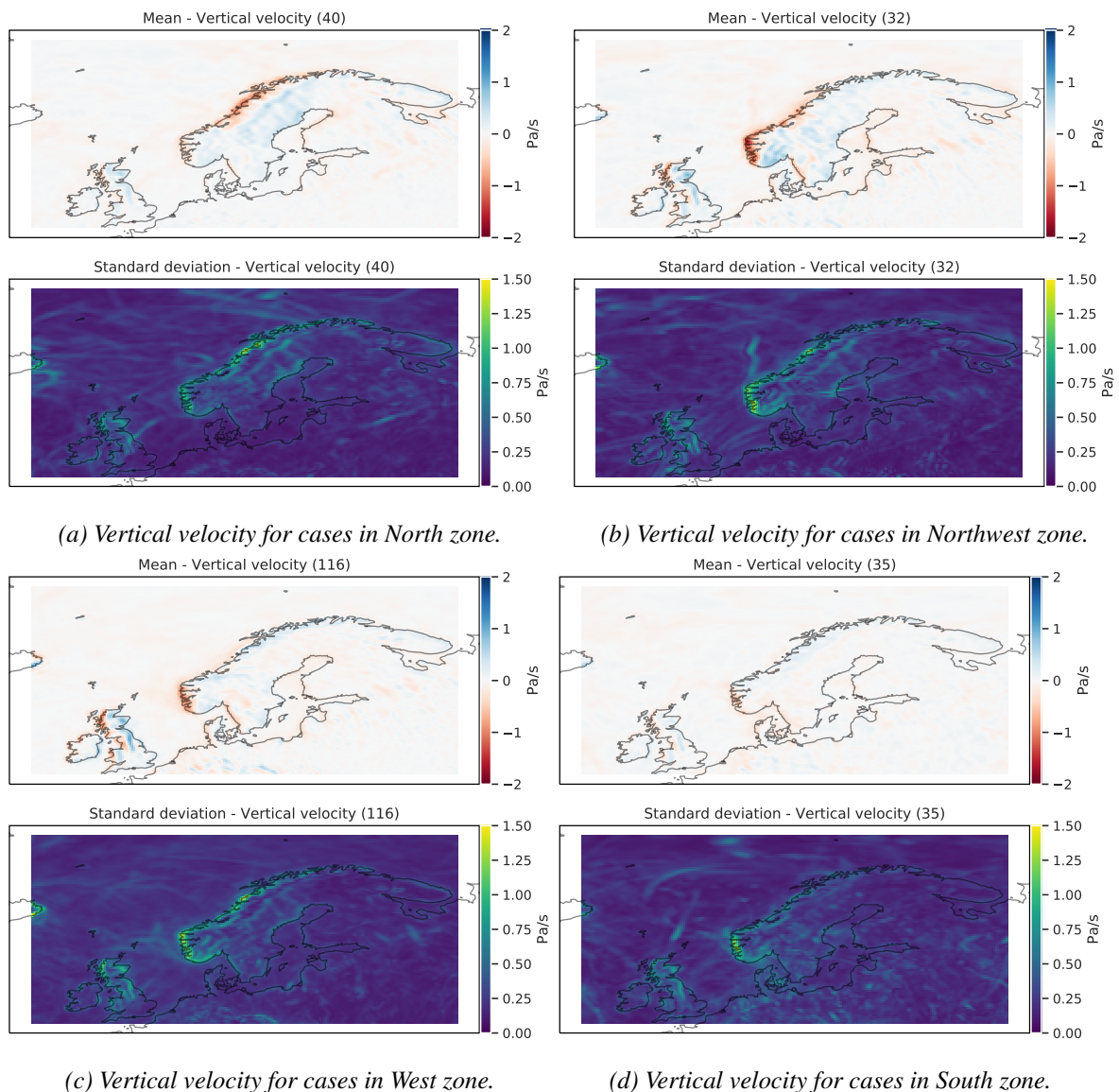
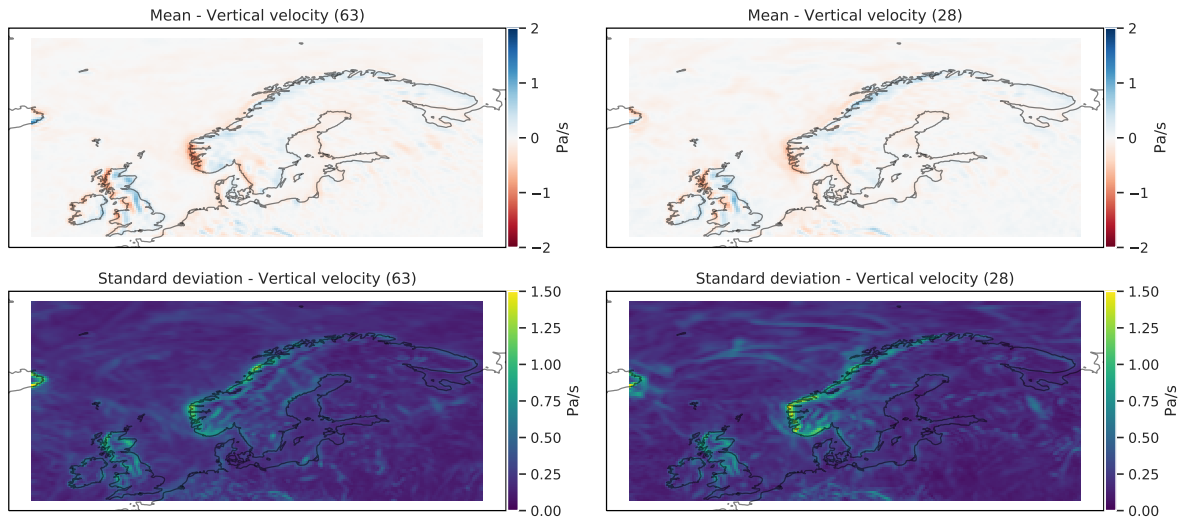
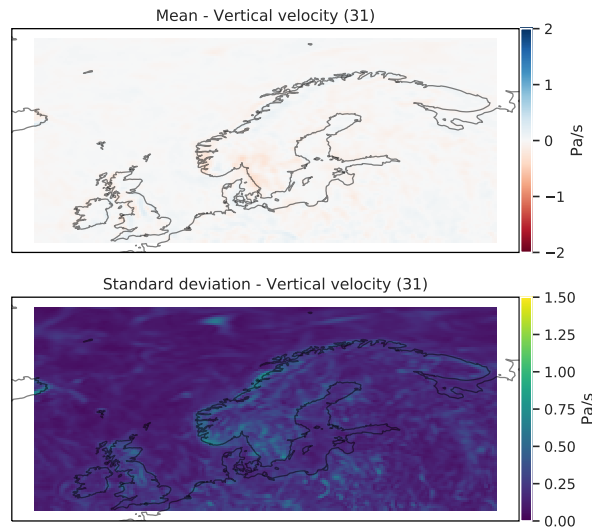


Figure 4.10: Vertical velocity composites for both HTL and FwTL cases in different geographical zones. Included are only cases for which height information was provided in the Avinor data set. The velocity was found by interpolating to the correct height as described in Section 3.5



(a) Vertical velocity for cases at Flesland

(b) Vertical velocity for cases at Sola



(c) Vertical velocity for cases in Gardermoen zone.

Figure 4.11: Same as Figure 4.10, but for only the biggest airports.

#### 4.2.5 Different types of precipitation for triggered lightning events

The ERA5 reanalysis model differentiates between convective precipitation arising from the convection scheme in the integrated forecasting system and large scale precipitation arising from the cloud scheme in the integrated forecasting system. To investigate the atmospheric conditions, this thesis divides into these two different categories of precipitation to distinguish between large scale and locally caused precipitation.

##### Large scale precipitation

Figure 4.12 shows no clear sign of large scale precipitation being present anywhere but the west coast of Norway. However, for *all* the composites (all zones), only the west coast has substantial amounts of large scale precipitation. This is further reinforced when looking at

## 4.2. METEOROLOGICAL PHENOMENA RELATED TO TRIGGERED LIGHTNING

the case for Flesland and Sola in Figure 4.13. Again, Gardermoen sticks out due to not having any clear sign of large scale precipitation neither at the west coast nor around Gardermoen. This can again be explained by Gardermoen predominantly having triggered lightning events during summertime.

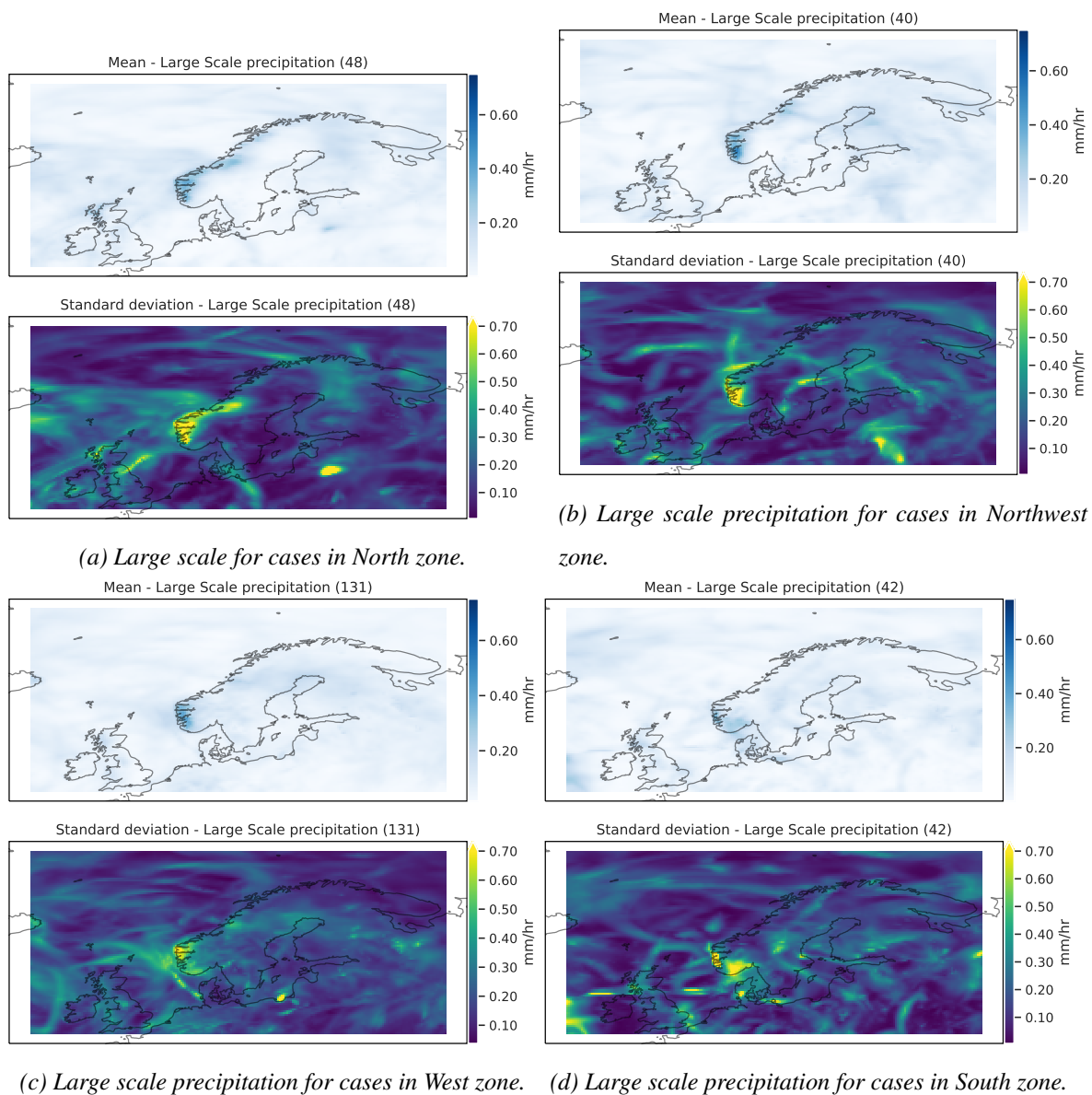
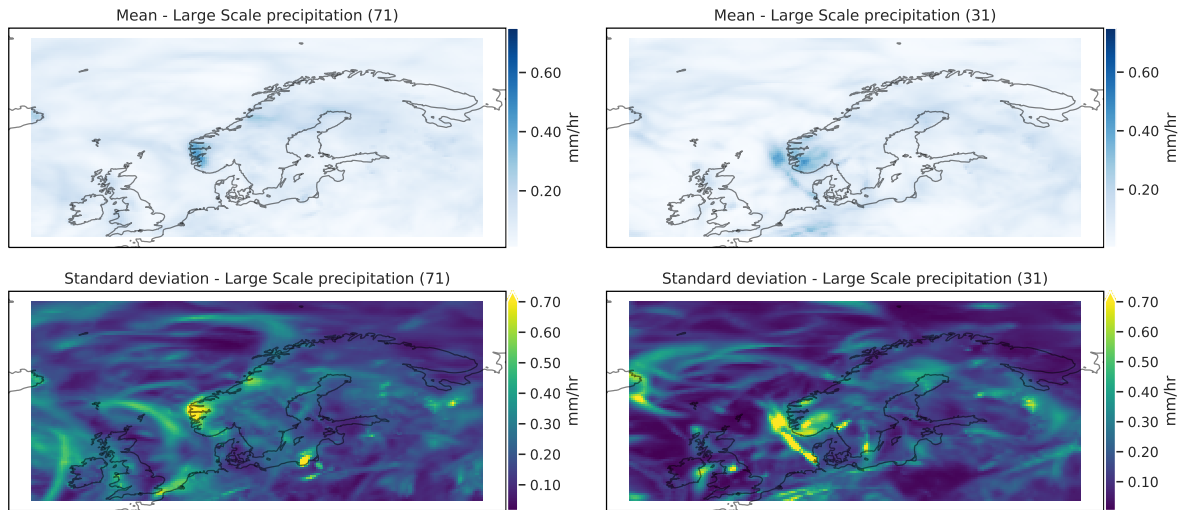
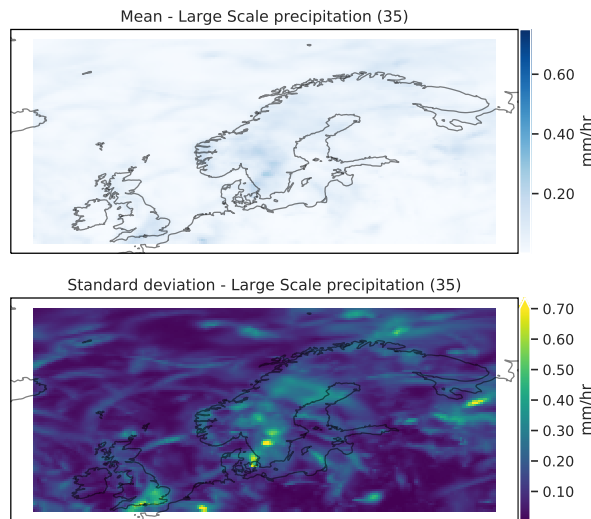


Figure 4.12: Large scale precipitation composites for both HTL and FwTL cases in different geographical zones. Included are cases where height information was not provided in the Avinor data set.



(a) Large scale precipitation for cases at Flesland. (b) Large scale precipitation for cases at Sola.



(c) Large scale precipitation for cases at Gardermoen.

Figure 4.13: Same as for Figure 4.12, but for only the biggest airports

### Convective precipitation

Now, considering the convective precipitation as shown in Figure 4.14, there are clear convective systems precipitating in all zones, even in the South zone. The standard deviation is also somewhat high, but this is to be expected when considering the chaotic nature of convective precipitation. This standard deviation is also higher than the mean value in some cases, which also hints to a problem of placing convective scale systems, as was the case for the coastal zones discussed in Section 4.2.4. The cases near the airports are shown in Figure 4.15. Flesland and Sola show the same picture as the previous figure in that there is a large precipitation intensity along the west coast, but high standard deviation, especially around Sola in the Sola case and around Flesland in the Flesland case. Here, Gardermoen also has

## 4.2. METEOROLOGICAL PHENOMENA RELATED TO TRIGGERED LIGHTNING

very clearly convective precipitation related to the triggered lightning events.

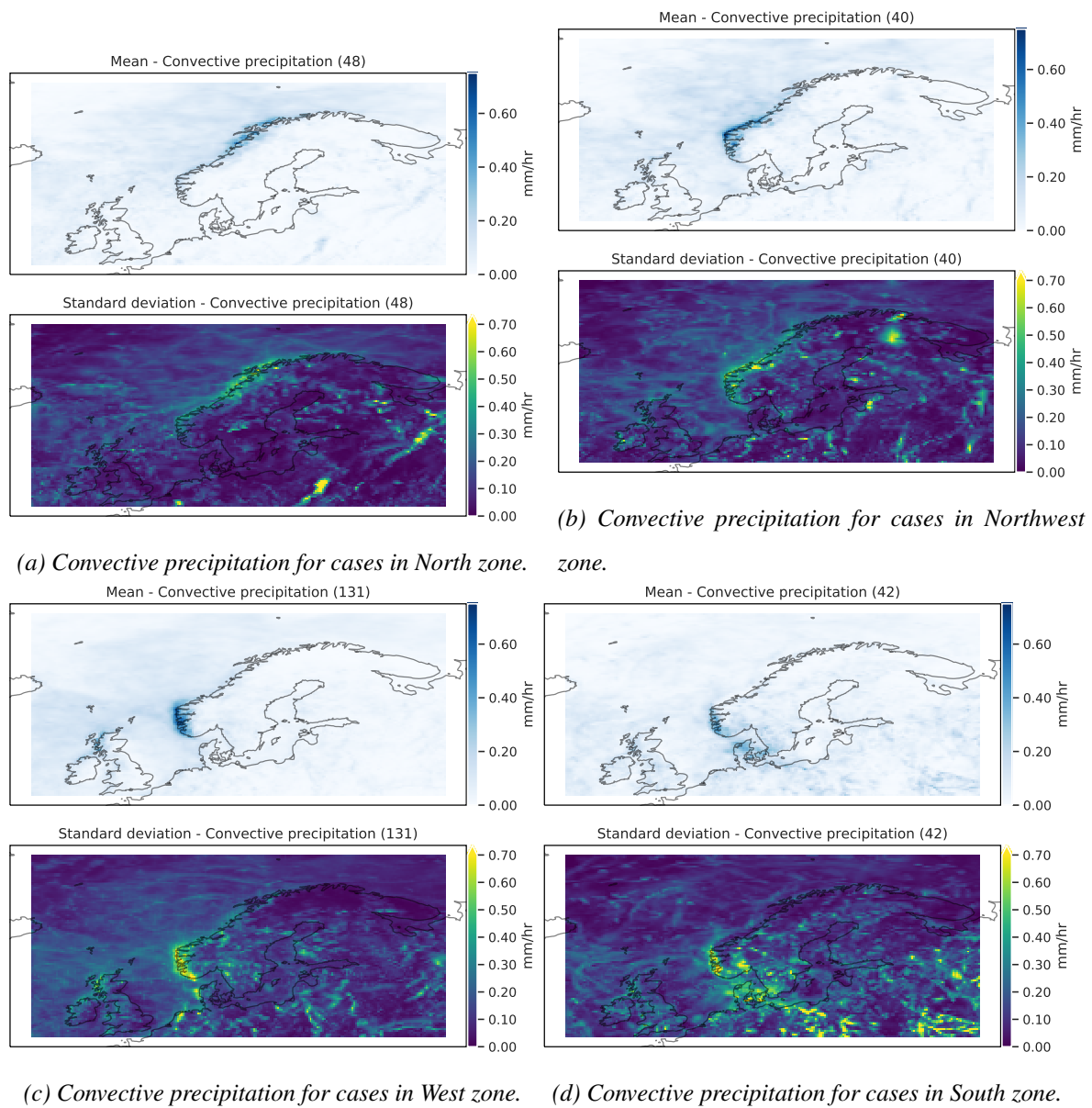
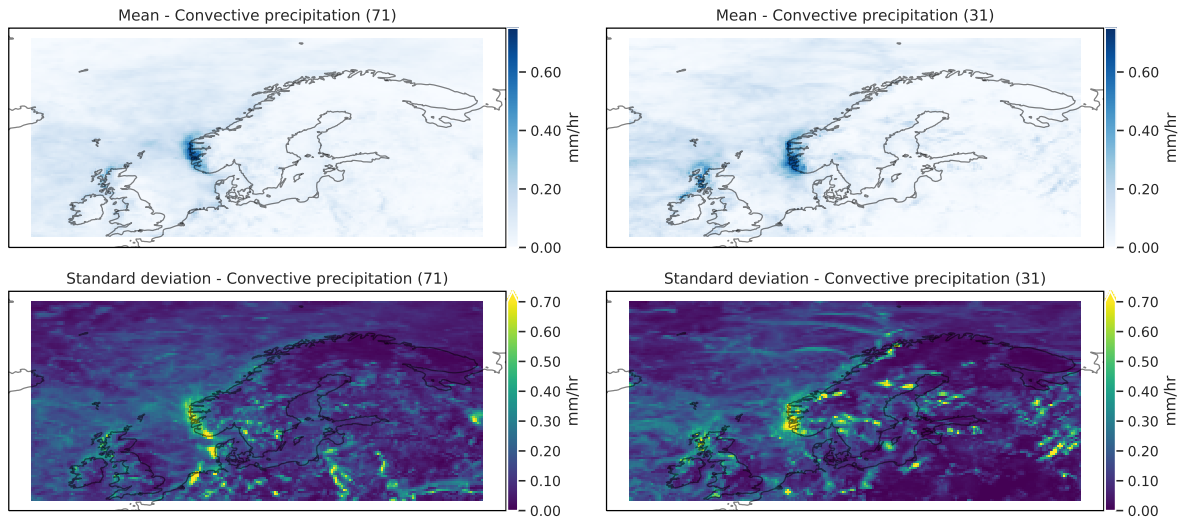
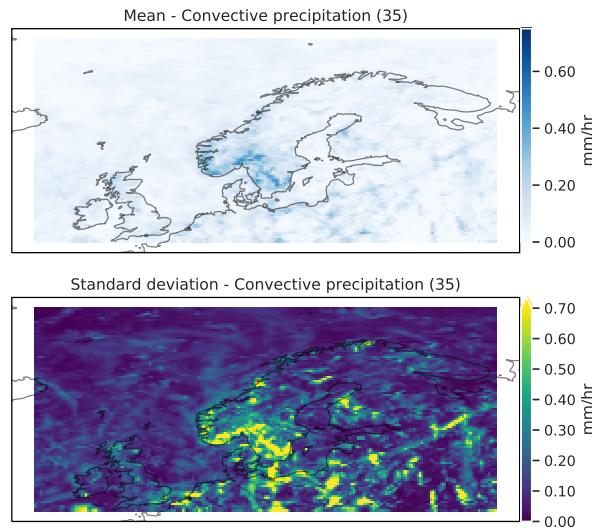


Figure 4.14: Convective precipitation composites for the different zones



(a) Convective precipitation for cases at Flesland

(b) Convective precipitation for cases at Sola



(c) Convective precipitation for cases in Gardermoen zone.

Figure 4.15: Convective precipitation composites for the biggest airports.

#### 4.2.6 Why are there more HTL near Flesland than near Sola?

Looking at the flight traffic data compared to triggered lightning events in Table 4.1, it is clear that Flesland airport has the highest incident per traffic ratio of the large Norwegian airports. Figure 4.7 shows Flesland to have a higher (20%) frequency of rain than Sola at 15%. The same is seen for both categories of showers (*SH*, *VCSH*). This suggests a more convective area around Flesland airport than at Sola airport. Ørlandet has similar convective activity to Flesland, but has almost no commercial air traffic. Therefore, any triggered lightning incident would not be in this data set and there is a smaller amount of potential trigger events.

### 4.3. IMPLICATIONS OF PRECIPITATION ERROR IN HTI

This convective difference between Flesland and Stavanger cannot be explained by yearly traffic differences, and their geographical positions are so close that there should not be any substantial climatological temperature differences between the two. There is somewhat less lightning activity observed at Flesland compared to Sola. As discussed in 4.2.3, the local topography seems to be important for triggered lightning incidents. As such Flesland airport is situated among mountains, whilst Sola airport is in a flatter area.

	Sola (ENZV)	Flesland (ENBR)	Gardermoen (ENGM)
Average yearly traffic (2016-2018)	74 532	92 128	253 599
Lightning close to airport (2008-2019)	30 920	22 774	68 321
Cases close to airport	24	63	35
Case per traffic	1 / 31 055	1 / 14 624	1 / 72 457
Case per recorded lightning	1 / 1 289	1 / 361	1 / 1 952

Table 4.1: Average traffic, accumulated lightning activity, and cases within  $0.5^\circ$  ( $\approx 50\text{km}$ ) radius of the three biggest Norwegian airports.

### 4.3 Implications of precipitation error in HTI

As stated in Section 2.6.1, an error has been found in the usage of precipitation data when forecasting HTI. The error was usage of *accumulated* precipitation instead of *hourly* precipitation in the forecast. A complete case-by-case effect of this is shown in the figures in Appendix A. Figure 4.16 shows the effect of considering hourly instead of accumulated precipitation<sup>1</sup>. Shown is an approximate halving of the frequency of Yellow risk for all airports. The higher risk categories (Orange and Red) are only substantially reduced at northfacing airports, i.e. airports in the northwest and North zone. Sola and Flesland see a halving in the Orange category, but not a substantial reduction in the Red. Flesland and Sola have approximately the same frequency of Red and Orange forecasts, but as shown in 4.1, Flesland has double the amount of HTL and FwTL cases.

To further investigate whether this leads to any reduction in HTI forecast skill, METAR data was considered to verify that HTI correctly identifies coastal and off-shore convective activity. Thus, the effect for the three airports from the North zone are shown in Figure 4.17. The figure shows a clear increase in frequency of non-White risk categories for all three airports. Hammerfest and Bodø have a slight increase in HTL-related phenomena forecasted as

<sup>1</sup>Maps showing the effect for the whole domain are moved to Appendix A



White (Here, snow and showers.) However, there is also some reduction in other phenomena such that this seems to be a non-substantial increase. The same is observed for Figure 4.18, which shows the risk categories for the three northwestern coastal airports: a clear increase in frequency of non-White risk categories when convective activity is observed. It should be noted that there seems to be no clear total increase or decrease in the White category for all three airports. In all, the skill of the HTI does not seem to be reduced, but rather increased by taking into account the hourly precipitation.

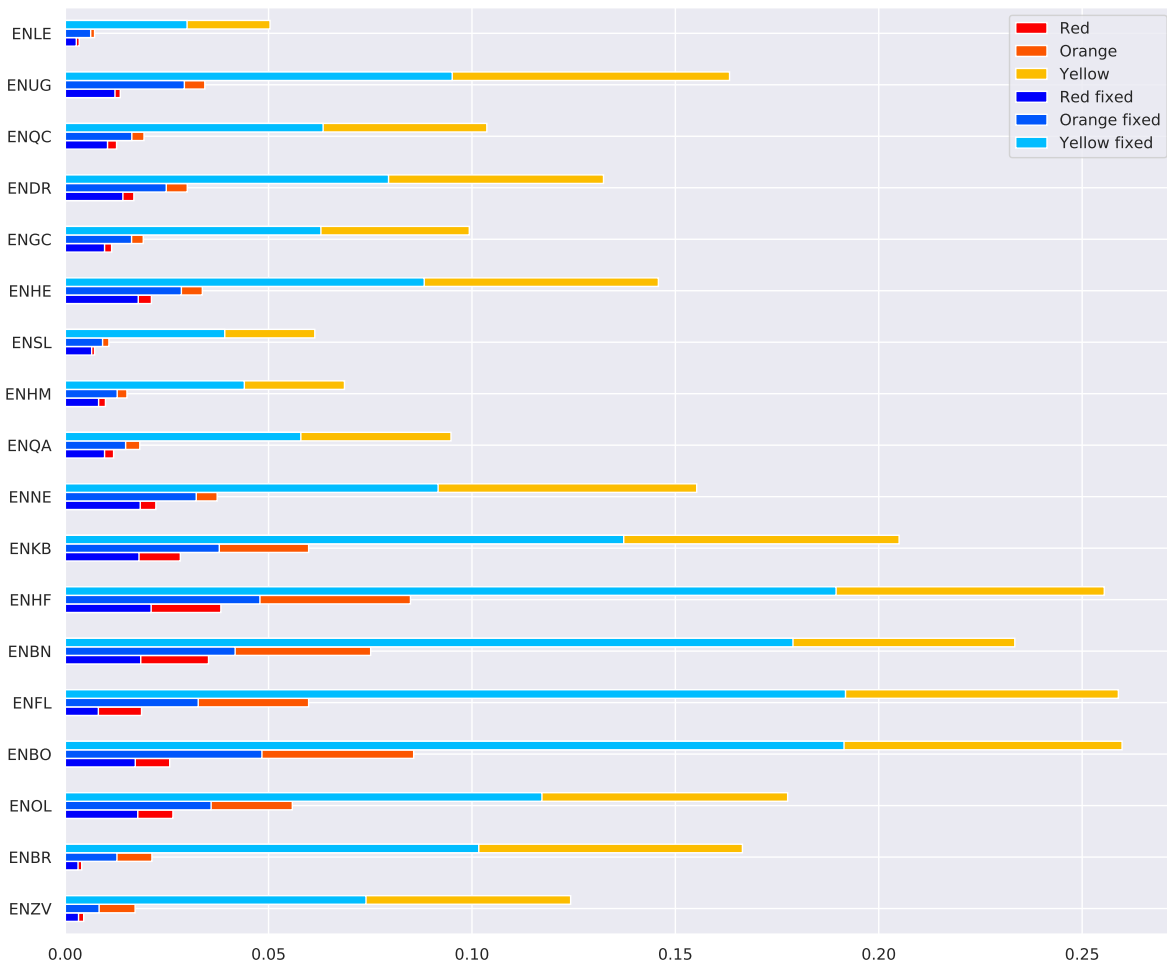


Figure 4.16: Frequency of HTI-risk levels during HTL-season (October-April), before and after fixing the erroneous forecast, for selected airports.

### 4.3. IMPLICATIONS OF PRECIPITATION ERROR IN HTI

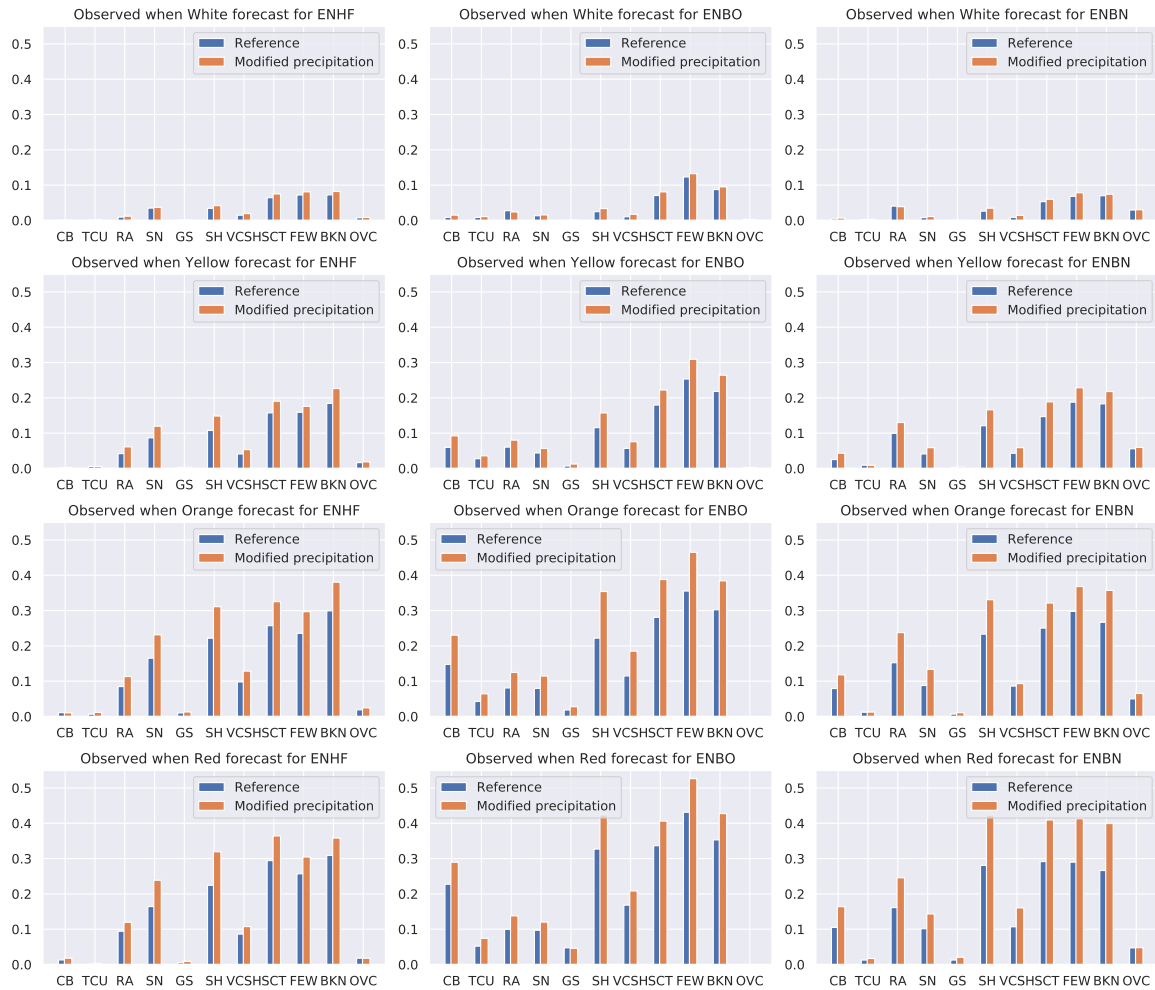


Figure 4.17: Frequency of HTI-risk given observed meteorological-phenomenon during HTL-season (October-April), for the three northernmost coastal airports: Hammerfest (ENHF), Bodø (ENBO), and Brønnøysund (ENBN)

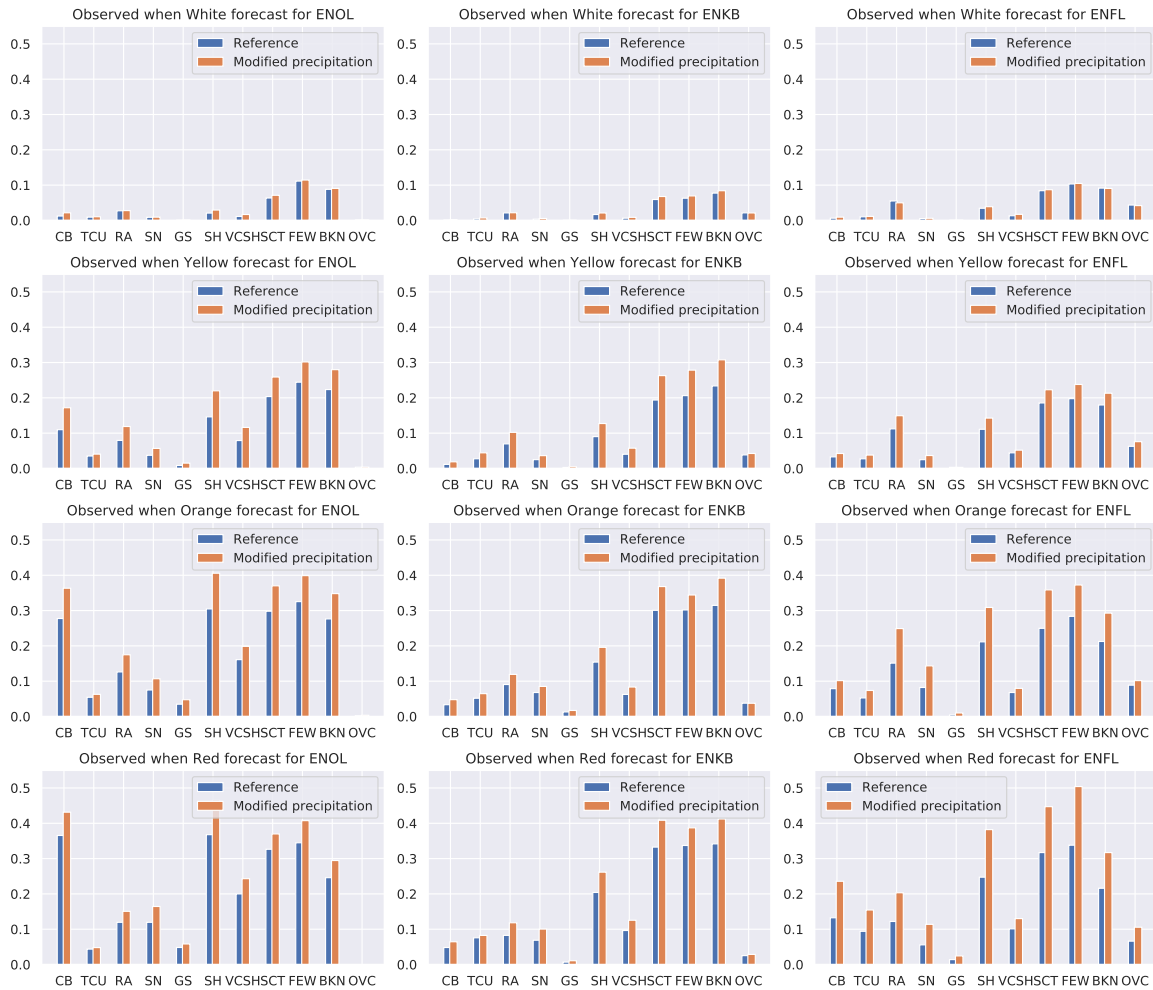


Figure 4.18: Frequency of HTI-risk given observed meteorological-phenomenon during HTL-season (October-April), for the three northwestern coastal airports: Ørlandet (ENOL), Kristiansund (ENKB), and Florø (ENFL)

## 4.4 Decompositional analysis of triggered lightning incidents

As discussed in Section 3.4, calculating sub-indices of forecasted HTI during recorded incidents allows for investigation into which, if any, of the sub-indices was under-evaluating the HTI risk. As stated in Section 2.6, HTI is calculated to be representative for the 750m ( $\approx$  2500 feet) altitude. Thus, the following discussion only pertains to what is forecast at this altitude, and not (necessarily) at the height of the incident, as was done in Section 4.2.2.

Figure 4.19 shows 11 HTL cases from the Avinor data set with the sub-indices stacked on top of each other. On the x-axis is the altitude (in feet) at which the helicopter was flying. The figure shows the HTI to be at least 0.5 for all 11 cases, but no cases were forecasted as Red

#### 4.4. DECOMPOSITIONAL ANALYSIS OF TRIGGERED LIGHTNING INCIDENTS

---

and only two cases were forecasted as Orange. This is summarized in Table 4.2. Figure 4.20 shows the sub-indices clearly delineated so that one can see which of the indices are lacking. The temperature sub-index is full for all but the third case, which, when calculated, had a temperature of  $-0.67^{\circ}\text{C}$ . Increasing the temperature to full would not increase the risk level in this case. Further, it can also be seen that in two of the 11 cases, precipitation would have been reduced to almost 0 if hourly instead of accumulated precipitation was considered, thus reducing the risk level to White. The third case where precipitation would be almost 0, was already White, so a reduction in risk level would not be seen. The most variability is found in the cloud and vertical velocity parameters. It should be noted that vertical velocity has had a positive value for all the cases, meaning that the upper threshold of the vertical velocity sub-index may be too strict. The cloud parameter reduces the risk level substantially (from Red to Yellow) for four of the cases.

Looking now at the Fixed wing cases in 4.21, which shows the total HTI decomposed to the sub-indices, with the altitude of the aircraft in feet on the x-axis. It can be seen that ten of the 34 cases would have a reduction in HTI due to consideration of the hourly (and not accumulated) precipitation. Only for three cases would this give a decrease in risk level. Even though some of these fixed wing incidents are happening at higher altitudes (e.g. 7000 feet), we see a relatively high sub-index for some of them, suggesting that there may be some convective activity in the whole column. This is also summarized in Table 4.3. Looking at Figure 4.22, one can see that vertical velocity is non-zero for *all* cases, showing the vertical velocity to be positive in the case of triggered lightning events - even though many cases might be situated above or below the 750m altitude. The precipitation sub-index is generally not affected by differing heights, since it is a measure of how much precipitation would reach the ground - not precipitation in each level. The temperature sub-index shows a somewhat bad relation to the FwTL. 19 of the cases had zero contribution from the temperature. This could be solely due to the aircraft being situated above or below the 750m altitude, but still close to the  $0^{\circ}\text{C}$  isotherm.

It is to be noted from Tables 4.2 and 4.3 that even though four fixed wing cases were correctly identified as Red, 41% were below the Yellow threshold. For the helicopter cases, zero were correctly identified as Red, but only two of the 11 (18.2%) were below the Yellow threshold. Further, the helicopter data set is heavily influenced by the fact that they were recorded after the operational forecasting started: Any Red events were warned against and helicopter pilots

have had an increased participation and reporting during this period. This may have lead to a skewing of the data set towards the tail of the majority of the cases, as seen in Figure 4.2, where the helicopter cases do not have a peak at the expected 0°C isotherm.

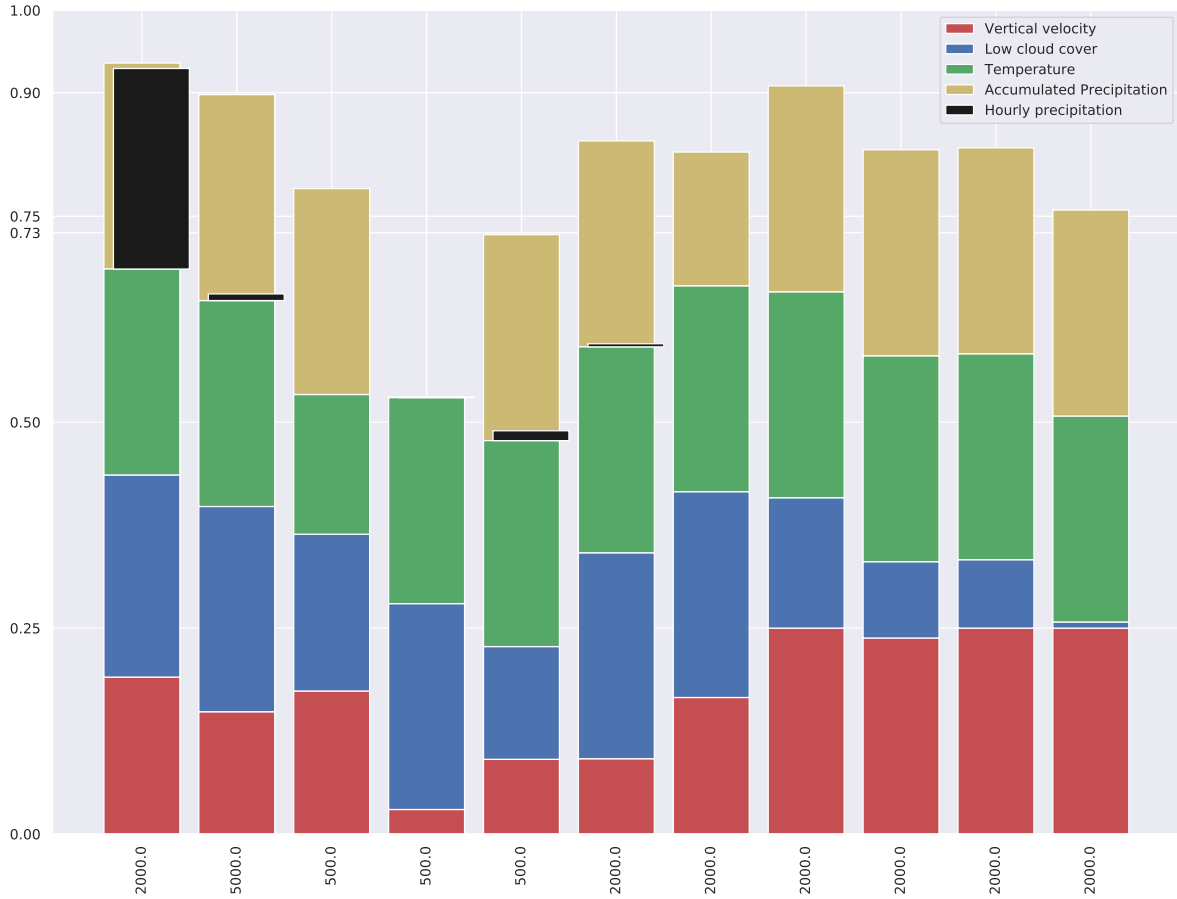


Figure 4.19: Contributions from the different sub-indices, for Helicopter cases during the operational forecast. X-axis is height of incident in feet. Black on yellow is correction made by using the hourly precipitation instead of accumulated precipitation. Included are only cases from Avinor data set where position and height was available, for cases after November 2016.

Forecast	With Accumulated	Without Accumulated	Missed (%)
>Yellow (0.73)	9	7	2 (18.2%)
>Orange (0.90)	2	2	7 (63.6%)
>Red (0.99)	0	0	11 (100%)

Table 4.2: Amount of cases forecast in each risk category based on the 11 Helicopter cases in Figure 4.19. A Red risk is counted in Orange, and Yellow.

#### 4.4. DECOMPOSITIONAL ANALYSIS OF TRIGGERED LIGHTNING INCIDENTS

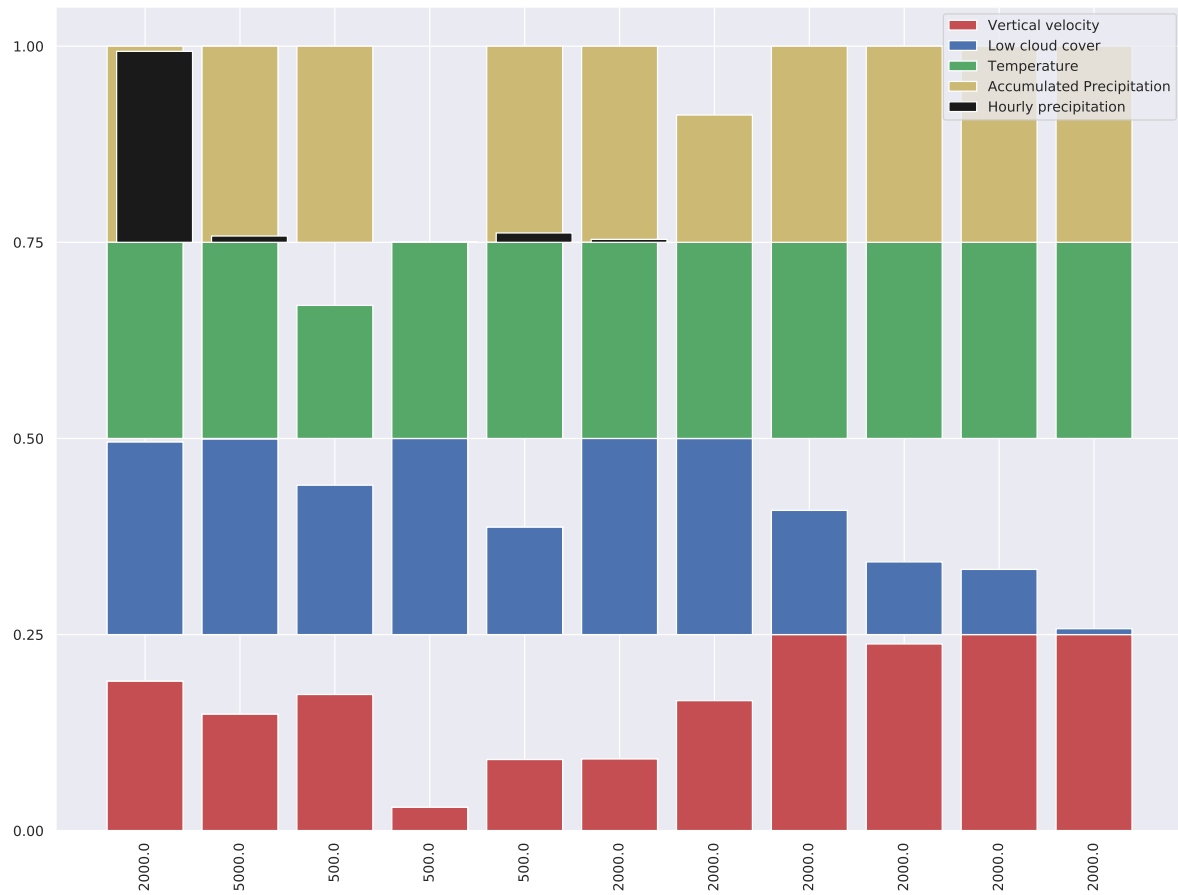


Figure 4.20: Same as 4.19, but clearly delineated between the sub-indices

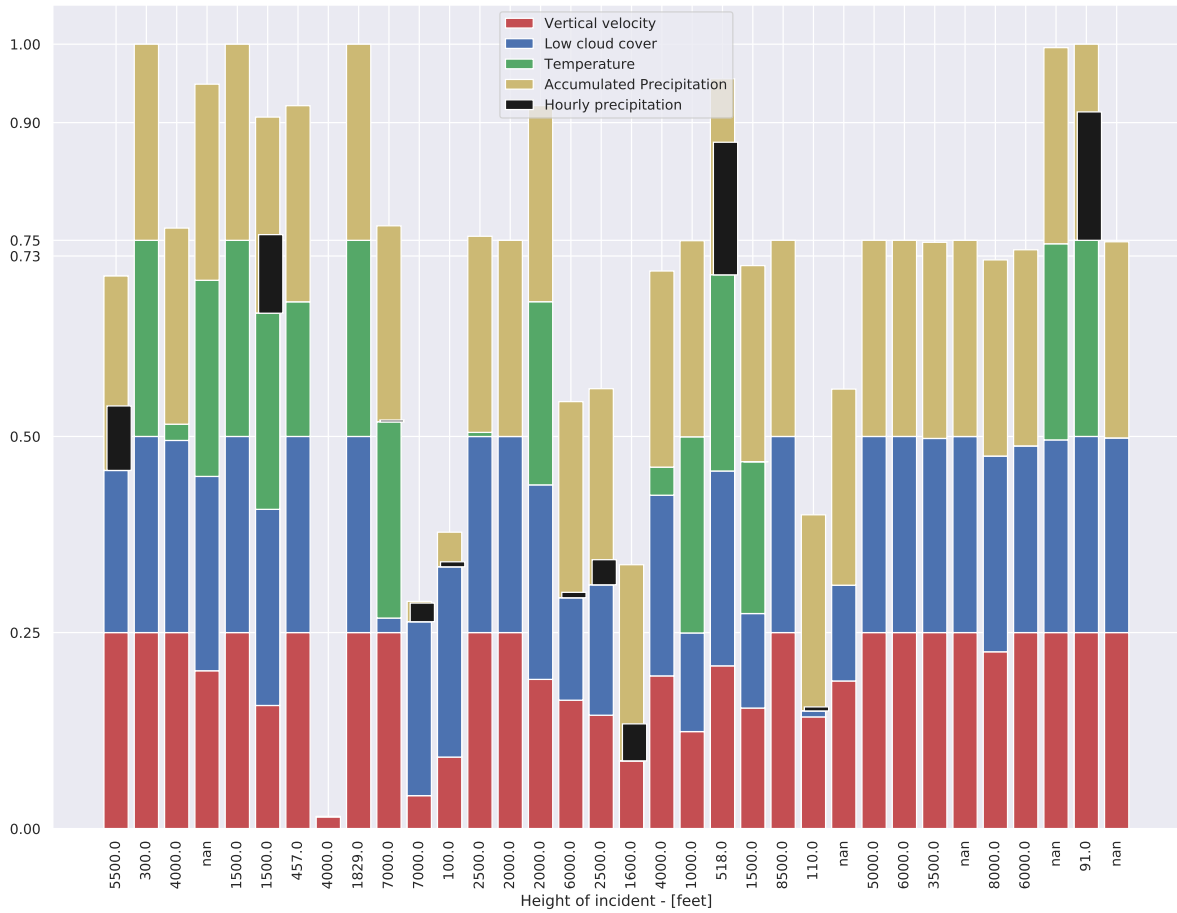


Figure 4.21: Contributions from the different sub-indices, for Fixed wing cases during the operational forecast. X-axis is height of incident in feet. Black on yellow is correction made by using the hourly precipitation instead of accumulated precipitation. Included are only cases from Avinor data set where position and height was available, for cases after November 2016.

Forecast	With Accumulated	Without Accumulated	Missed
>Yellow (0.73)	22	21	14 (41.2%)
>Orange (0.90)	10	8	25 (73.5%)
>Red (0.99)	4	3	30 (88.2%)

Table 4.3: Amount of cases forecast in each risk category based on the 34 Fixed wing cases in Figure 4.21. A Red risk is counted in Orange, and Yellow.

#### 4.4. DECOMPOSITIONAL ANALYSIS OF TRIGGERED LIGHTNING INCIDENTS

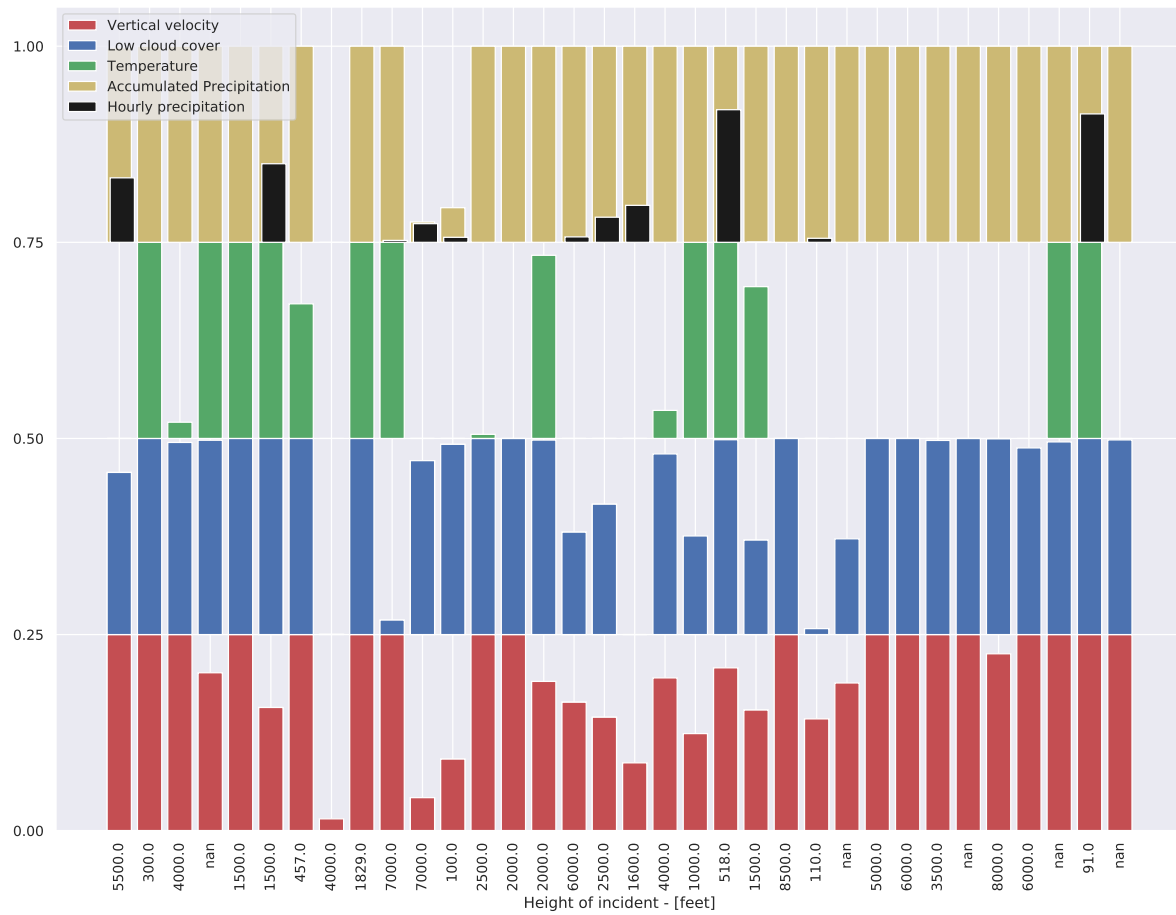


Figure 4.22: Same as 4.21, but clearly delineated between the sub-indices



# 5 Conclusions

## 5.1 Are there still cases of Helicopter Triggered Lightning in Norway?

Helicopter Triggered Lightning is still a recurring phenomenon, even after several years of forecasting the Helicopter Trigger Index. This is the reason why it is necessary to continue researching the phenomenon - the ideal scenario would be a forecast which prevented such cases altogether.

This thesis found there to be an increase in cases in Norway after forecasting began in 2016. However, this may be seen as an artificial increase, as helicopter operators were in direct dialogue with the Meteorological Institute and more interested in reporting cases in order to improve the forecasting ability. It should also be noted that during the forecast period there have been no *major* incidents. The cases happening were also found to be happening at lower temperatures than the expected  $0^{\circ}\text{C}$  isotherm. This was discussed in Section 4.1: It is probably the result of forecasting removing the theoretical peak at  $0^{\circ}\text{C}$ , where more major incidents would have happened.

## 5.2 What meteorological phenomena are present during triggered lightning incidents?

To identify atmospheric conditions leading to HTL, both METAR and composite plots were studied. This thesis found from both METAR and composite plots that convective precipitation and non-stratiform cloud types are related to triggered lightning incidents. This thesis also reaffirms that the temperature during triggered lightning events were situated around  $-3$  to  $0^{\circ}\text{C}$  for the altitude of the aircraft, both for the fixed wing and for the helicopter situation. It also found typical pressure patterns leading to geostrophic winds incident on coastal areas, suggesting convection due to ocean-land roughness effects being an important factor in triggered lightning incidents. This ocean-land roughness effect may also contribute to Flesland having more triggered lightning incidents than Sola, due to Flesland being surrounded by more mountainous landscape.

## **5.3 In what ways can the HTL forecast be improved?**

By implementing a decomposition strategy, this thesis found the precipitation and temperature sub-indices in the Helicopter Trigger Index to be quite good at forecasting HTL. The vertical velocity sub-index along with the cloud sub-index may have reduced the risk level from Red to Yellow in seven of the 11 cases studied.

These results imply that improvements can be made to the HTI by weighting the precipitation and temperature sub-indices. Also, a reduction in the upper threshold of the vertical velocity criteria should be considered, as there is present a positive vertical velocity in all the recorded triggered lightning incidents.

By reintroducing the hourly precipitation, there seems to be no severe risk increase, but rather a skill increase of the HTI forecast, such that an implementation of this fix would improve the forecast ability. This thesis was not able to perform an investigation into whether ensemble systems were able to increase the forecast skill, though preliminary efforts into this is expected to help in cases where precipitation was missing. There is also a known underestimation of coastal precipitation in the MEPS system, such that investigations into increasing the precipitation threshold should be done when this known underestimation has been corrected. Lastly, including the  $0^{\circ}\text{C}$  isotherm in the operational forecast should be considered, but further sensitivity tests are necessary. As discussed in Section 3.6.2, the current interpolation scheme for the temperature is for a coarse vertical area based on the findings of Wilkinson et al., 2013. Investigations into improving this by using model level interpolation instead of the current pressure levels may give increased ability, as the difference in case temperatures between the finer ERA5 pressure levels and coarser MEPS pressure levels were substantial.

# A Additional figures

## A.1 HTI before and after fix of erroneous forecast

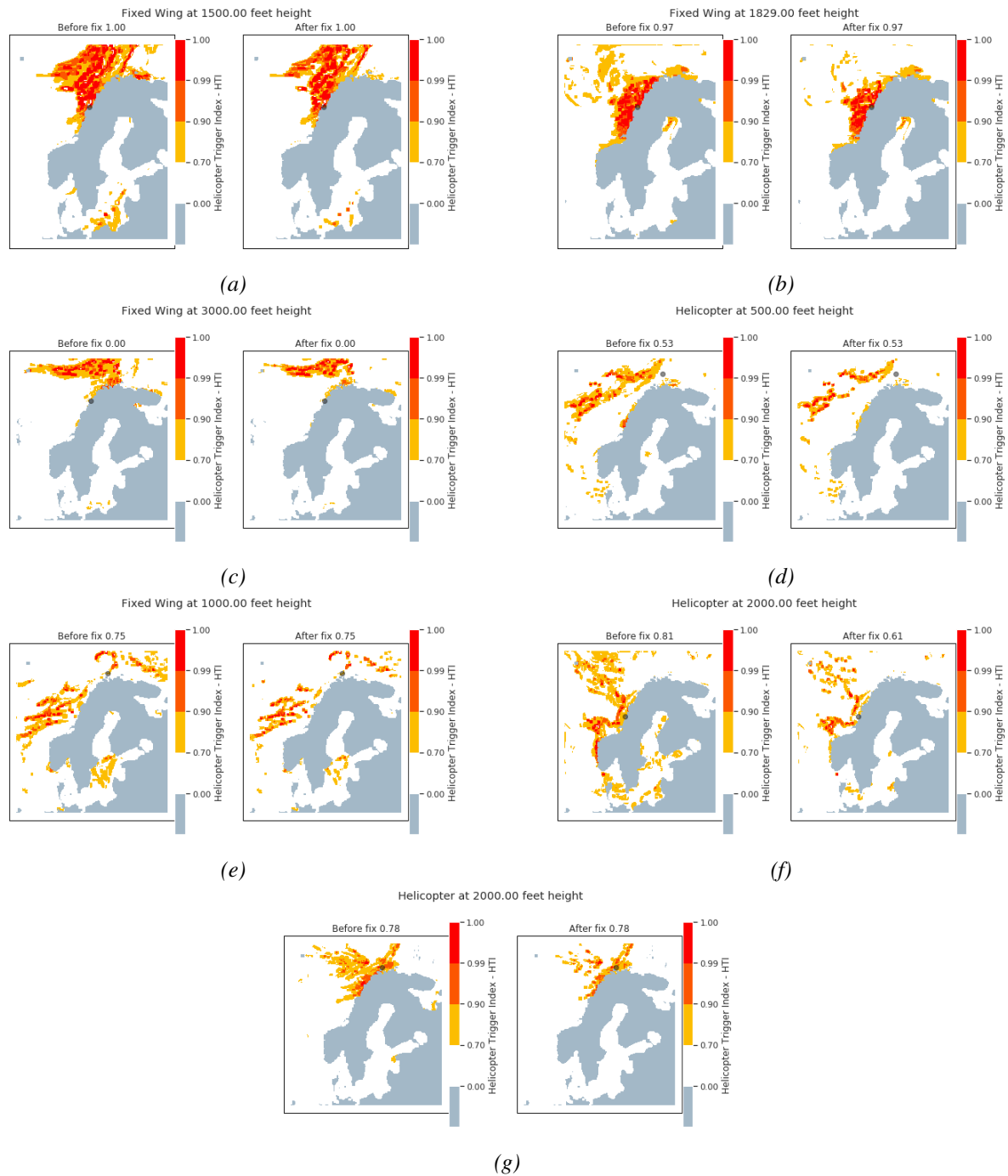


Figure A.1: North zone, cases with HTI-value before and after precipitation change

## A.1. HTI BEFORE AND AFTER FIX OF ERRONEOUS FORECAST

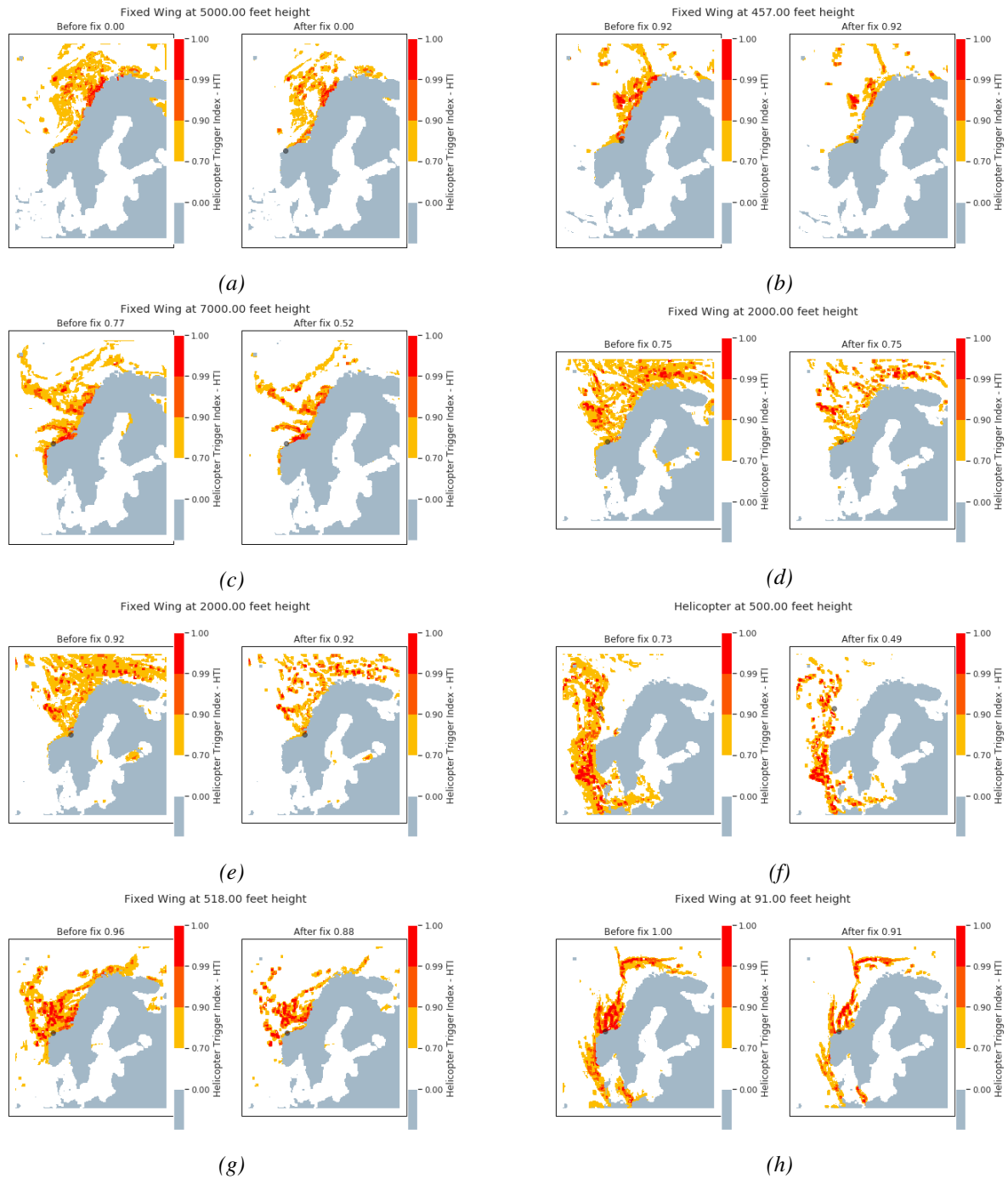


Figure A.2: North West zone, cases with HTI-value before and after precipitation change

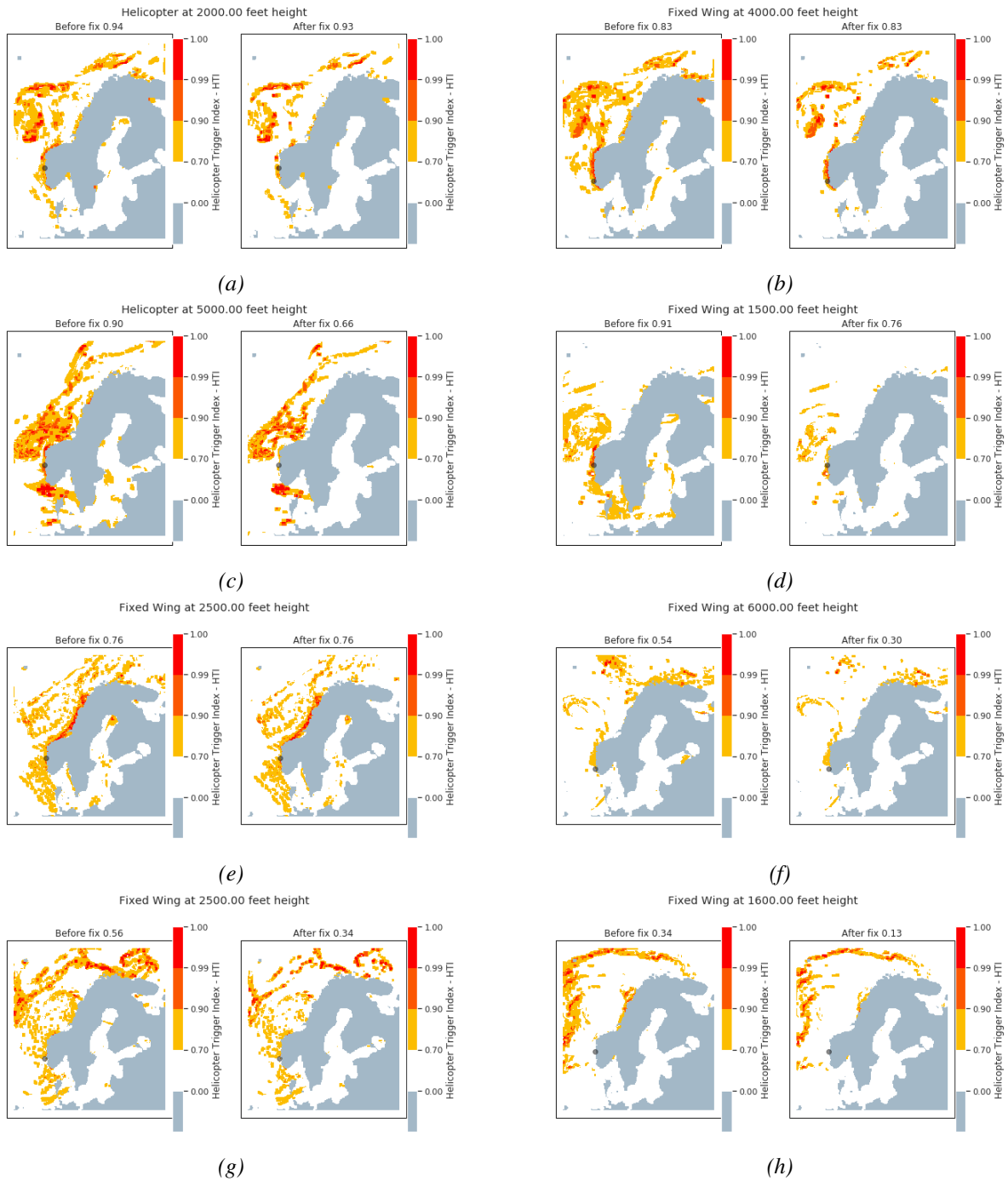


Figure A.3: West zone (First part), cases with HTI-value before and after precipitation change

## A.1. HTI BEFORE AND AFTER FIX OF ERRONEOUS FORECAST

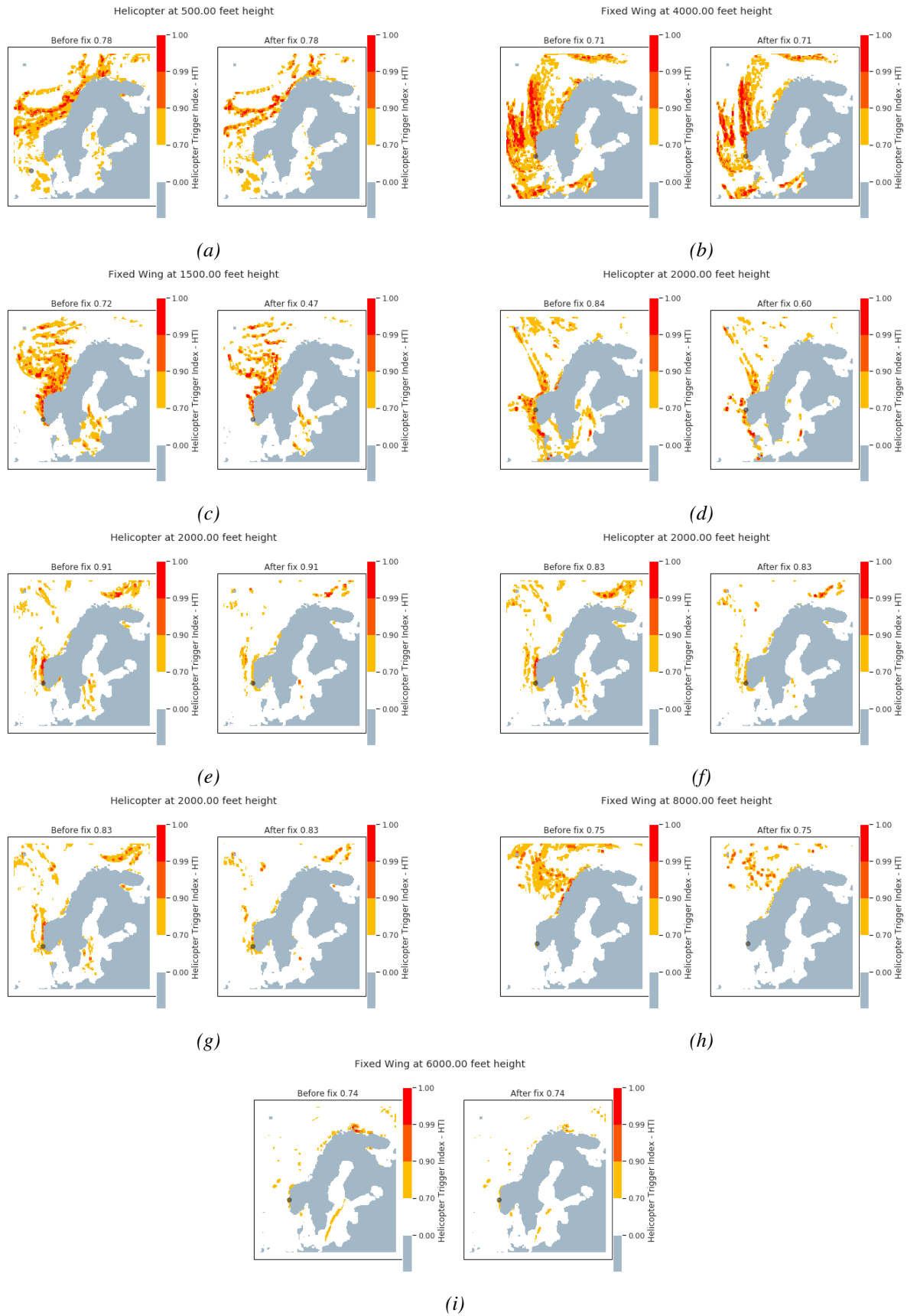


Figure A.4: West zone (Second part), cases with HTI-value before and after precipitation change

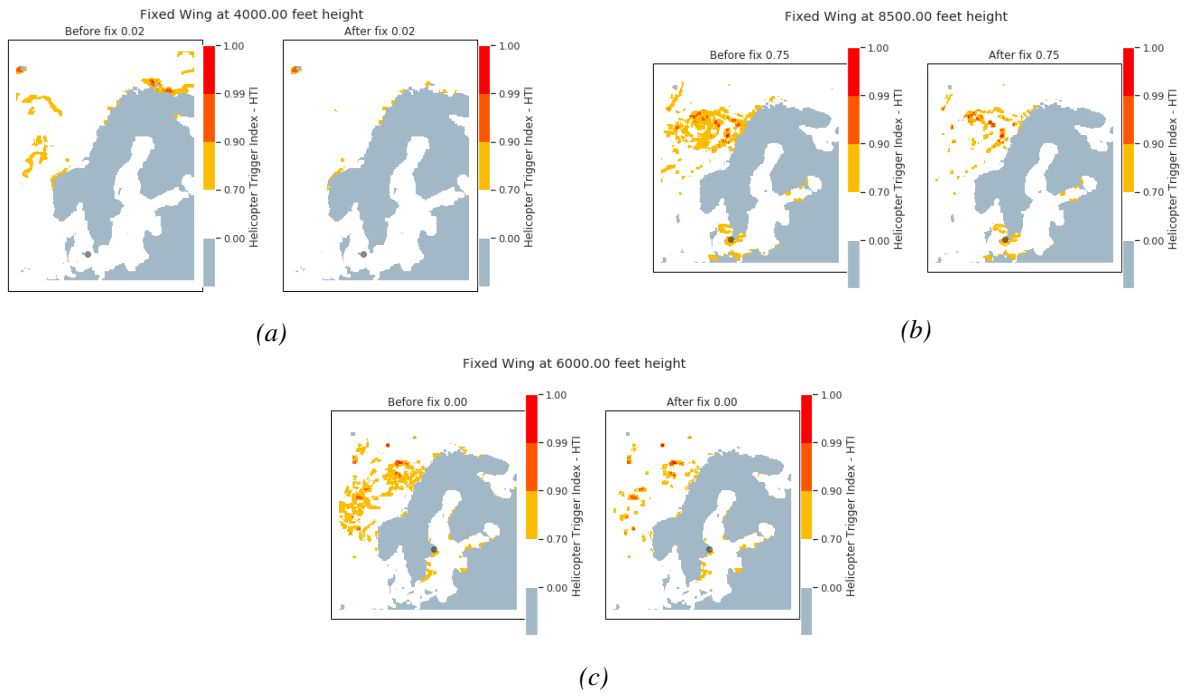


Figure A.5: South zone, cases with HTI-value before and after precipitation change

## A.1. HTI BEFORE AND AFTER FIX OF ERRONEOUS FORECAST

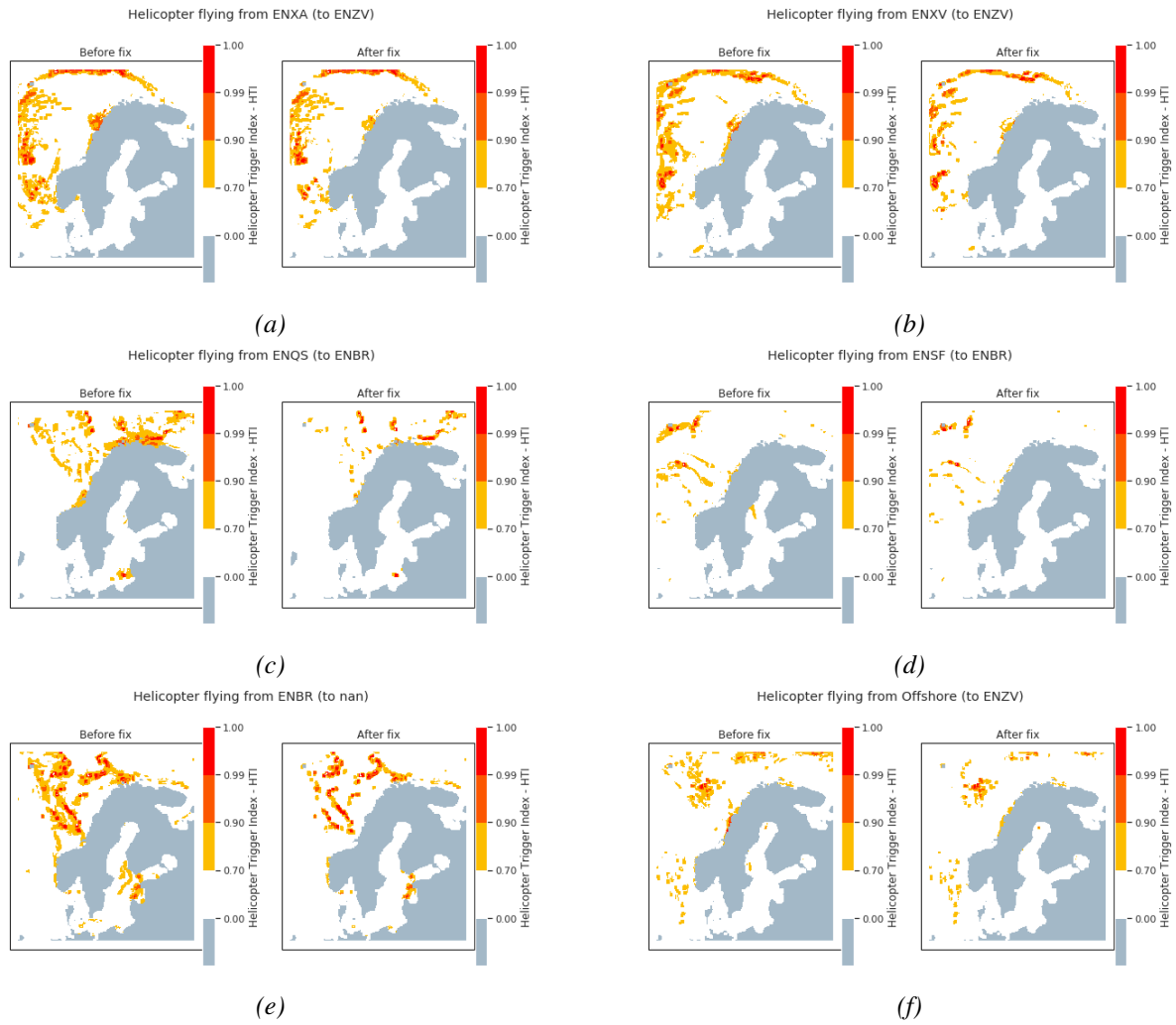


Figure A.6: Cases where exact position is not-known, with HTI-value before and after precipitation change



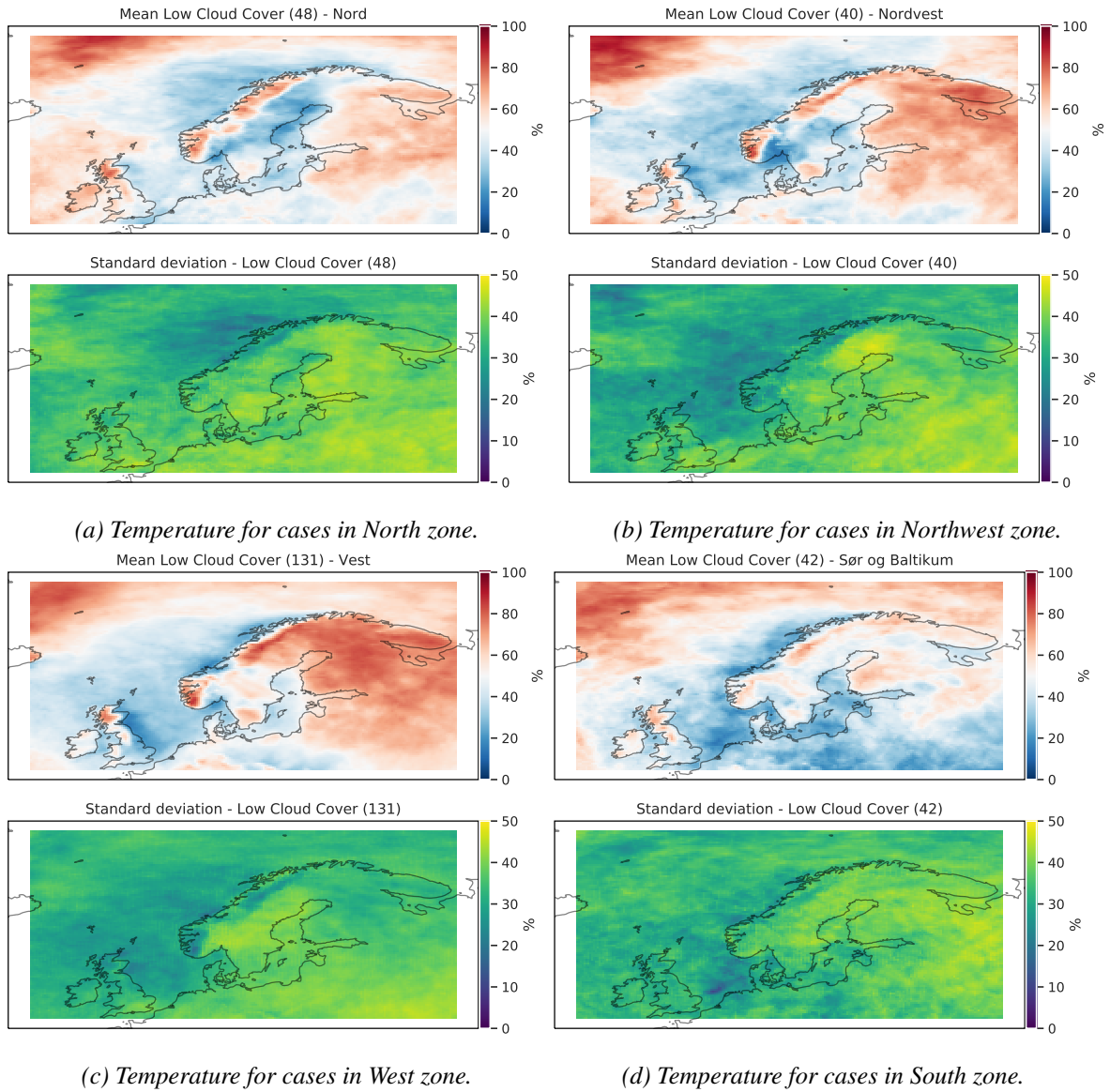
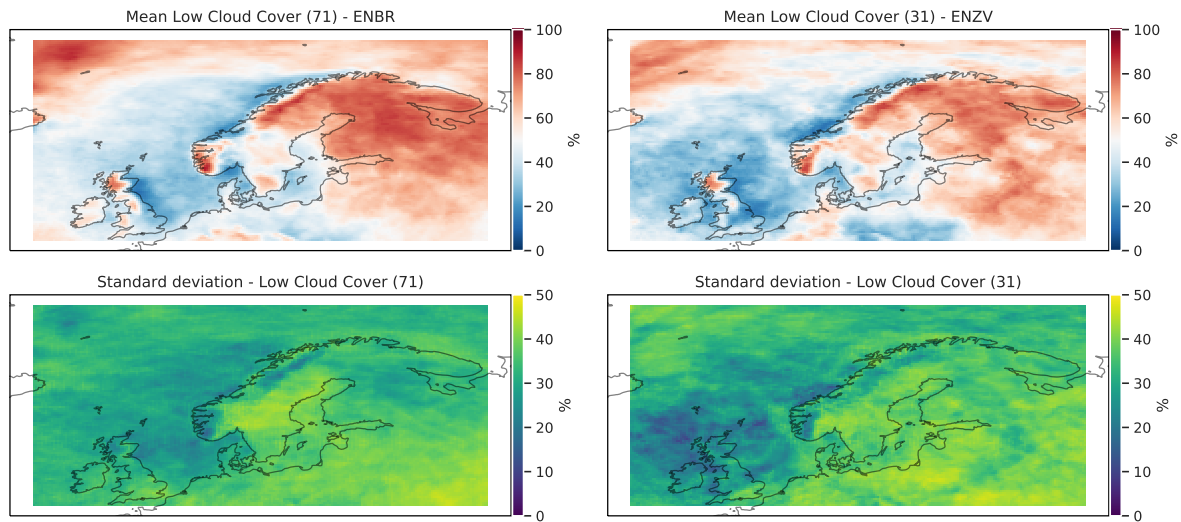


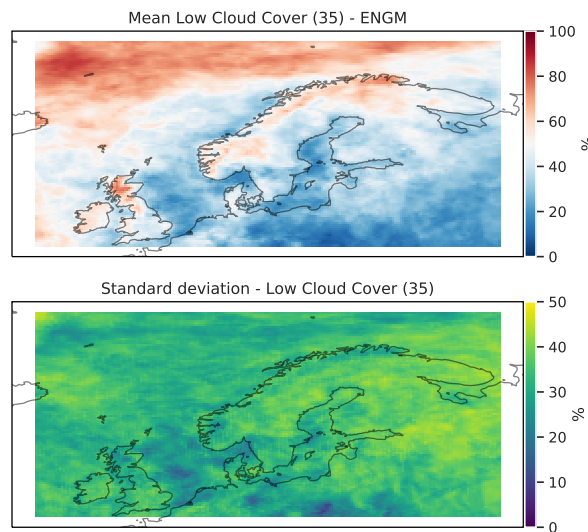
Figure A.7: Cloud cover composites for both HTL and FwTL cases in different geographical zones. Included are cases where height information was not provided in the Avinor data set.

## A.1. HTI BEFORE AND AFTER FIX OF ERRONEOUS FORECAST



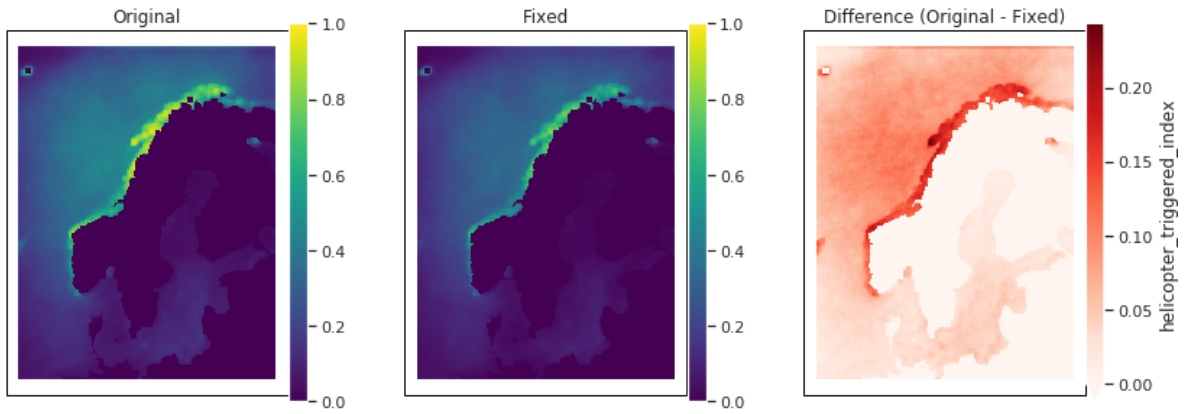
(a) Cloud cover for cases at Flesland

(b) Cloud cover for cases at Sola

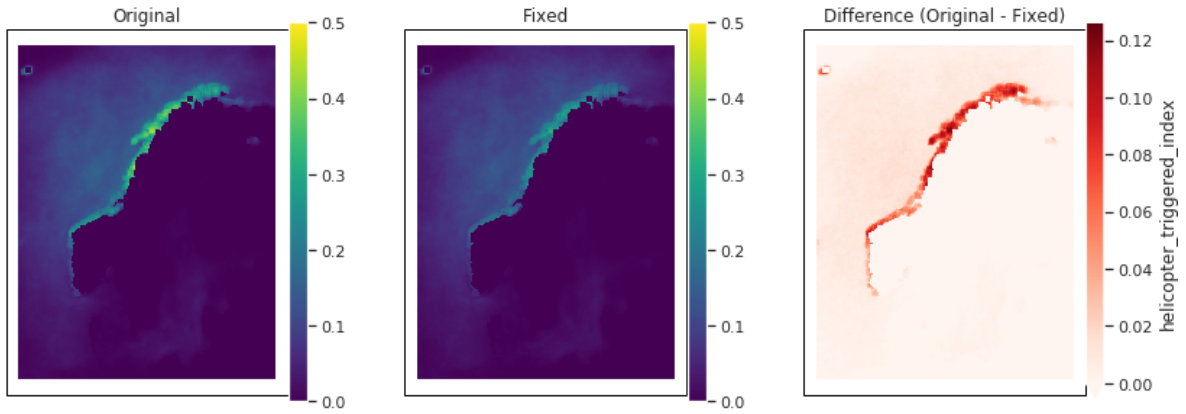


(c) Cloud cover for cases at Gardermoen.

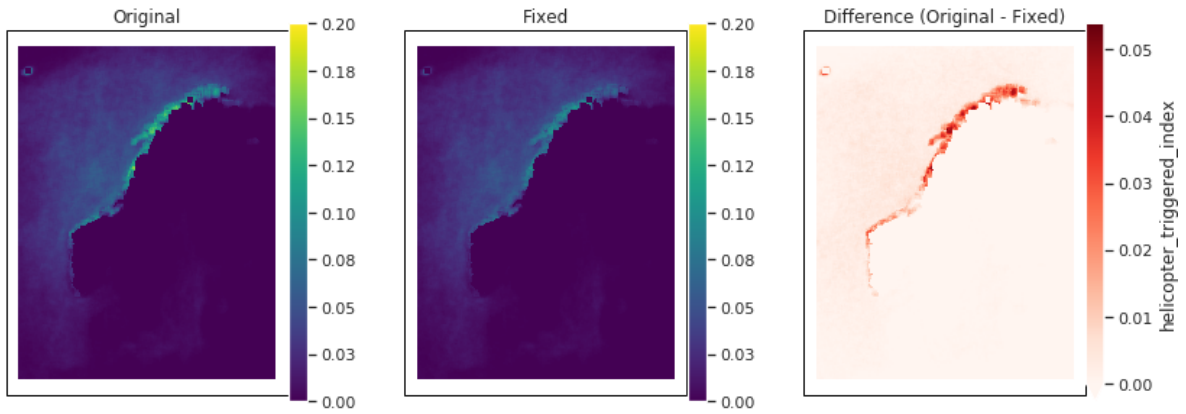
Figure A.8: Cloud cover composites for both HTL and FwTL cases for only the biggest airports. Included are cases where height information was not provided in the Avinor data set.



(a) Frequency of Yellow risk levels before and after fixing the erroneous forecast



(b) Frequency of Orange risk levels before and after fixing the erroneous forecast



(c) Frequency of Red risk levels before and after fixing the erroneous forecast

Figure A.9: Frequency of the different risk levels of HTI during HTL-season (October-April), before and after correction of erroneous use of accumulated precipitation. Also shown is the absolute difference between the original and fixed frequencies.

## Helicopter Triggered Lightning

### Procedures HTI

This table has been adapted by all helicopter Operators on the Norwegian Shelf

This table is also published in the OM A

Please notice that the required "action" differs between Night and Day

Colour code	Risk	Action
Red	High	Do not plan Flights into Red areas
Brown	Medium	Enter these areas subject to the following conditions. <ul style="list-style-type: none"> <li>Maintain at least 10 NM from CB cells</li> <li>Avoid heavy precipitation by continuous use of weather radar enroute</li> <li>If possible maintain VMC below cloud base</li> <li>Avoid wherever safe to do so, the temperature band between -2°C and +2°C</li> <li>At least 5% additional contingency fuel shall be carried</li> </ul> <b>NOTE:</b> During hours of Night, Brown shall be considered Red, and procedures for Red should be followed.
Yellow	Low	No restrictions, but proper caution towards actual conditions (CB's, heavy precipitation, temperature) that may contribute to Triggered Lightning should be exercised. <b>NOTE:</b> During hours of Night, Yellow shall be considered Brown, and procedures for Brown should be followed.





24

Figure A.10: Operational risk levels and description of procedures during reported risk for HTI. As reported to the helicopter operators. Note: Brown risk level has been consequently called Orange through the whole thesis.

## B Airport names and geographical zones

The airports have been grouped together to reduce noise in the composite plots as discussed in Section 3.3, the zones are shown in Figure B.1.

### B.1 ICAO-codes

ICAO-codes are airport identification codes determined by the International Civil Aviation Organization, ICAO. These are used to identify different airports in this thesis, and are tabulated in Table B.1.

ICAO-code	Airport name	ICAO-code	Offshore installation
ENGM	Gardermoen (Oslo)	ENXA	Ekofisk A
ENBR	Flesland (Bergen)	ENLE	Ekofisk L
ENZV	Sola (Stavanger)	ENXV	Varg
ENKB	Kvernberget (Kristiansund)	ENSF	Statfjord A
ENFL	Florø	ENQS	Statfjord C
ENBO	Bodø	ENUG	Goliat FPSO
ENBN	Brønnøy (Brønnøysund)	ENNE	Norne A
ENOL	Ørland	ENHE	Heidrun A
ENHF	Hammerfest	ENDR	Draugen
ENML	Årø (Molde)	ENQA	Troll A
ENHV	Valan (Honningsvåg)	ENGC	Gullfaks C
		ENHM	Heimdal
		ENSL	Sleipner A

Table B.1: ICAO-code for the airports and helipads used in this thesis.

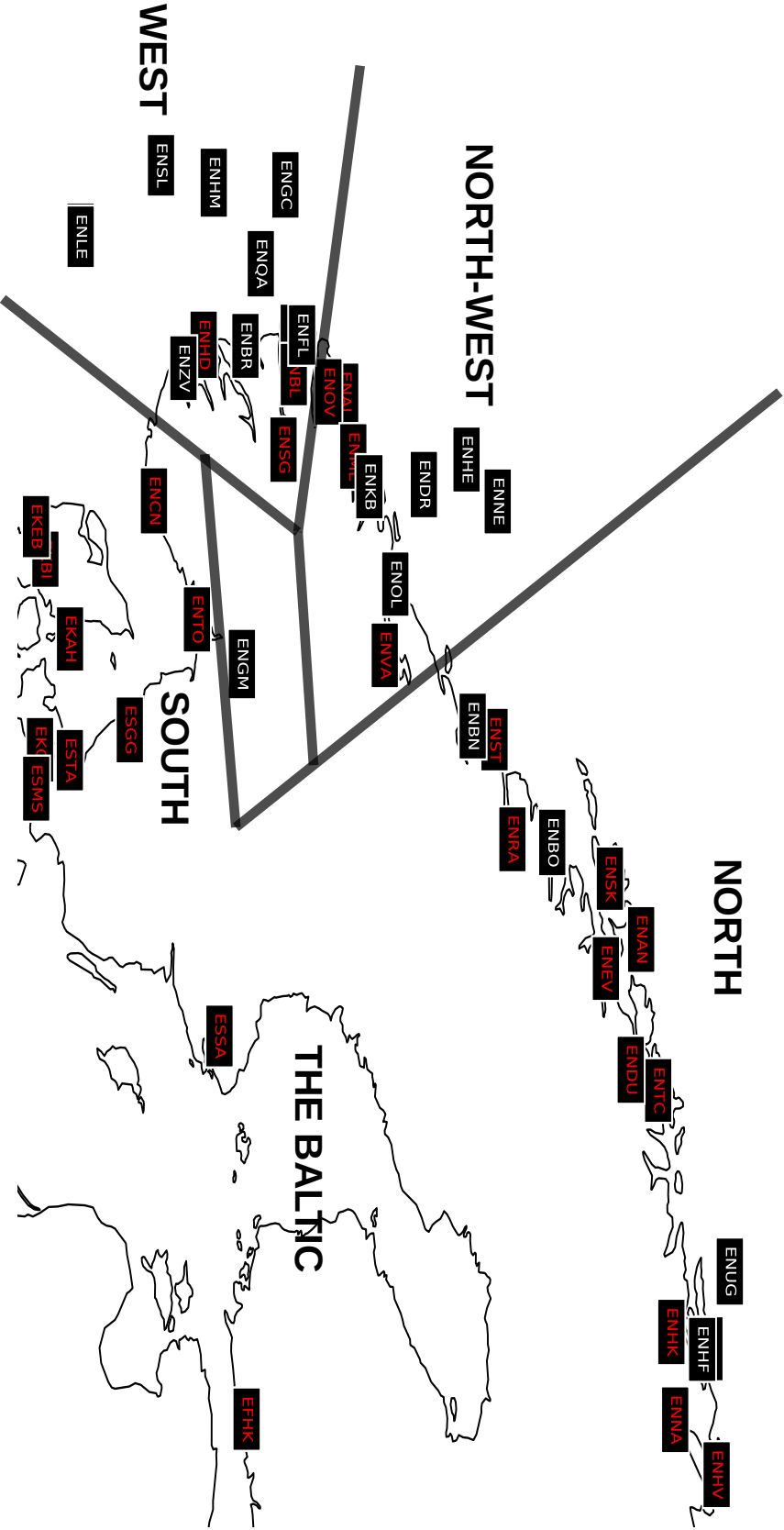


Figure B.1: Zones used in this thesis, with used METAR-stations in white, and airports with at least one incident in red.

# Bibliography

Bengtsson, Lisa, Ulf Andrae, Trygve Aspelien, Yurii Batrak, Javier Calvo, Wim Rooy, Emily Gleeson, Bent Sass, Mariken Homleid, Mariano Hortal, Karl-Ivar Ivarsson, Geert Lenderink, Sami Niemelä, Kristian Nielsen, Jeanette Onvlee, Laura Rontu, Patrick Samuelsson, Daniel Muñoz, Alvaro Subias, and Morten Køltzow (Feb. 2017). “The HARMONIE-AROME model configuration in the ALADIN-HIRLAM NWP system”. In: *Monthly Weather Review*, 145. DOI: 10.1175/MWR-D-16-0417.1.

Hardwick, C. J. (1999). *Assesment of lightning threat to north sea helicopters: Final report*. Tech. rep. 99007. Civil Aviation Authority.

Harrison, R.G. (2012). “The Carnegie Curve”. In: *Surv Geophys*, 34, pp. 209–232. DOI: <https://doi.org/10.1007/s10712-012-9210-2>.

Hersbach, H, P de Rosnay, B Bell, D Schepers, A Simmons, C Soci, S Abdalla, M Alonso-Balmaseda, G Balsamo, P Bechtold, P Berrisford, J-R Bidlot, E de Boissésón, M Bonavita, P Browne, R Buizza, P Dahlgren, D Dee, R Dragani, M Diamantakis, J Flemming, R Forbes, AJ Geer, T Haiden, E Hólm, L Haimberger, R Hogan, A Horányi, M Janiskova, P Laloyaux, P Lopez, J Munoz-Sabater, C Peubey, R Radu, D Richardson, J-N Thépaut, F Vitart, X Yang, E Zsótér, and H Zuo (Feb. 2018). “Operational global reanalysis: progress, future directions and synergies with NWP”. In: ERA Report Series, (27). DOI: 10.21957/tkic6g3wm.

Jeffery, C. A. and P. H. Austin (1997). “Homogeneous nucleation of supercooled water: Results from a new equation of state”. In: *Journal of Geophysical Research: Atmospheres*, 102(D21), pp. 25269–25279. DOI: 10.1029/97JD02243. eprint: <https://agupubs.onlinelibrary.wiley.com/doi/pdf/10.1029/97JD02243>. URL: <https://agupubs.onlinelibrary.wiley.com/doi/abs/10.1029/97JD02243>.

Kallay, Nikola, Jan Drzymala, and Ana Cop (2015). In: *Encyclopedia of of Surface and Colloid Science*.

## BIBLIOGRAPHY

---

- Køltzow, Morten, Andreas Dobler, and Siri Sofie Eide (Sept. 2018). “Lightning in Norway under a future climate”. In: METreport, (9).
- Lamb, Dennis and Johannes Verlinde (2011). *Physics and Chemistry of Clouds*. Cambridge University Press. ISBN: 9780521899109.
- Lande, Knut (1999). *Lightning Strikes on Helicopters - Effects, Detection and Avoidance*. Tech. rep. 1999-01-2398. SAE Technical Paper.
- Lynn, Barry H., Yoav Yair, Colin Price, Guy Kelman, and Adam J. Clark (2011). “Predicting Cloud-to-Ground and Intracloud Lightning in Weather Forecast Models”. In: DOI: 10.1175/WAF-D-11-00144.1.
- March, Victor, Joan Montanyà, Ferran Fabró, Oscar Van der Velde, David Romero, Glòria Solà, Modesto Freijo, and Nicolau Pineda (Sept. 2016). “Winter lightning activity in specific global regions and implications to wind turbines and tall structures”. In: DOI: 10.1109/ICLP.2016.7791447.
- Michimoto, Koichiro (Jan. 2007). “Meteorological Aspects of Winter Thunderstorms along the Hokuriku Coast of Japan”. In: *IEEJ Transactions on Power and Energy*, 127, pp. 1242–1246. DOI: 10.1541/ieejpes.127.1242.
- Petrov, N.I., A. Haddad, G.N. Petrova, H. Griffiths, and R.T. Waters (2012). “Study of Effects of Lightning Strikes to an Aircraft”. In: *Recent Advances in Aircraft Technology*. Ed. by Ramesh K. Agarwal. Rijeka: IntechOpen. Chap. 22. DOI: 10.5772/36634. URL: <https://doi.org/10.5772/36634>.
- Pinatti, D. and S. Mascarenhas (1967). “Electrical Currents Produced during the Solidification of Water (Costa Ribeiro Effect)”. In: *Journal of applied physics*, 38 (6).
- Rakov, Vladimir A. and Martin A. Uman (2003). *Lightning: Physics and Effects*. Cambridge University Press. DOI: 10.1017/CB09781107340886.
- Saunders, C. P. R., H. Bax-norman, C. Emersic, E. E. Avila, and N. E. Castellano (2006). “Laboratory studies of the effect of cloud conditions on graupel/crystal charge transfer



- in thunderstorm electrification”. In: *Quarterly Journal of the Royal Meteorological Society*, 132 (621), pp. 2653–2673. DOI: 10.1256/qj.05.218. eprint: <https://rmets.onlinelibrary.wiley.com/doi/pdf/10.1256/qj.05.218>. URL: <https://rmets.onlinelibrary.wiley.com/doi/abs/10.1256/qj.05.218>.
- Saunders, C.P.R. (June 2008). “Charge Separation Mechanisms in Clouds”. In: *Space Sci. Rev.* 137, pp. 335–353. DOI: 10.1007/s11214-008-9345-0.
- Seibert, James (1962). *Helicopter static-electricity measurements*. Tech. rep. AD282087. US Army Transportation research command.
- (1972). *A fundamental study of static electric phenomena (Applied to Helicopters)*. Tech. rep. AD750617. United States army electronics command.
- Smart, Ken (1997). *Report on the accident to Aerospatiale AS332L Super Puma, G-TIGK, in North Sea 6nm south-west of Brae Alpha Oil Production Platform on 19 January 1995*. Tech. rep. 2. Department of the Environment, Transport and the Regions.
- (2005). *Report on the accident to Sikorsky S-76A+, G-BJVX near the Leman 49/26 Foxtrot platform in the North Sea 16 July 2002*. Tech. rep. 2. Department of Transport.
- Soula, S. (Dec. 2012). “Electrical Environment in a Storm Cloud”. In: *AerospaceLab*, (5), p. 1–10. URL: <https://hal.archives-ouvertes.fr/hal-01184322>.
- Stolzenburg, Maribeth, W. David Rust, and Thomas C. Marshall (1998). “Electrical structure in thunderstorm convective regions: 3. Synthesis”. In: *Journal of Geophysical Research: Atmospheres*, 103 (D12), pp. 14097–14108. DOI: 10.1029/97JD03545. eprint: <https://agupubs.onlinelibrary.wiley.com/doi/pdf/10.1029/97JD03545>. URL: <https://agupubs.onlinelibrary.wiley.com/doi/abs/10.1029/97JD03545>.
- Takahashi, Tsutomu, Takuya Tajiri, and Yasuo Sono (June 1999). “Charges on Graupel and Snow Crystals and the Electrical Structure of Winter Thunderstorms”. In: *Journal of the Atmospheric Sciences*, 56 (11), pp. 1561–1578. ISSN: 0022-4928. DOI: 10.1175/1520-0469(1999)056<1561:COGASC>2.0.CO;2. eprint: [https://journals.ametsoc.org/jas/article-pdf/56/11/1561/3440610/1520-0469\(1999\)056\\\_1561\\\_cogasc](https://journals.ametsoc.org/jas/article-pdf/56/11/1561/3440610/1520-0469(1999)056\_1561\_cogasc)

## BIBLIOGRAPHY

---

\_2\\_0\\_co\\_2 . pdf. URL: [https://doi.org/10.1175/1520-0469\(1999\)056%3C1561:COGASC%3E2.0.CO;2](https://doi.org/10.1175/1520-0469(1999)056%3C1561:COGASC%3E2.0.CO;2).

Toth, Zoltan and Eugenia Kalnay (Dec. 1993). “Ensemble Forecasting at NMC: The Generation of Perturbations”. In: *Bulletin of the American Meteorological Society*, 74 (12), pp. 2317–2330. ISSN: 0003-0007. DOI: 10.1175/1520-0477(1993)074<2317:EFANTG>2.0.CO;2. eprint: [https://journals.ametsoc.org/bams/article-pdf/74/12/2317/3726889/1520-0477\(1993\)074\\\_2317\\\_efantg\\\_2\\\_0\\\_co\\\_2.pdf](https://journals.ametsoc.org/bams/article-pdf/74/12/2317/3726889/1520-0477(1993)074\_2317\_efantg\_2\_0\_co\_2.pdf). URL: [https://doi.org/10.1175/1520-0477\(1993\)074%3C2317:EFANTG%3E2.0.CO;2](https://doi.org/10.1175/1520-0477(1993)074%3C2317:EFANTG%3E2.0.CO;2).

transport, Statens havarikommisjon for (2007). *Rapport om luftfartsulykke 4. desember 2003 på Bodø lufthavn med Dornier DO 228-202 LN-HTA, operert av Kato Airline AS*. Tech. rep. Statens Havarikommisjon for Transport.

Uman, M.A and Vladimir Rakov (Jan. 2003). “The interaction of lightning with airborne vehicles”. In: *Progress in Aerospace Sciences*, 39, pp. 61–81. DOI: 10.1016/S0376-0421(02)00051-9.

Wasilewska, Maja (2019). “Underøskelse av passasjerens risikopersepsjon i forbindelse med helikopterreise offshore”. MA thesis. University of Stavanger.

Wilkinson, Jonathan M, Helen Wells, Paul R Field, and Paul Agnew (2013). “Investigation and prediction of helicopter-triggered lightning over the North Sea”. In: *Meteorological Applications*, 20 (1), pp. 94–106. DOI: 10.1002/met.1314.

Williams, James P. Rydock; Earle R. (1991). “Charge separation associated with frost growth”. In: *Quarterly Journal of the Royal Meteorological Society*, 117 (498). DOI: 10.1002/qj.49711749809.